NTNU – Trondheim
Norwegian University of
Science and Technology

Estimation of Running Resistance in Train Tunnels

Muhammad Umer Nawaz

Project Management
Submission date: June 2015
Supervisor: Nils Olsson, IPK

Norwegian University of Science and Technology
Department of Production and Quality Engineering

Acknowledgment

Foremost, I would like to pay sincere gratitude to my suprevisor Prof. Nils Olsson for his continuous support, motivation, enthusiasm, and immense knowledge. This thesis was carried out at the Department of Production and Quality Egineering, in collaboration with Norges Statsbaner-NSB. Halvor Schrøder Hansen who is working as a Rådgiver at NSB, provided me with material, relevant data sets and guidance required for making this research work possible. His quest for performing high quality research was uplifting to me. I could not have imagined having a better supervision and mentors for my thesis.

My sincere thanks also goes to Brand Torben from Jernbaneverket for offering me the scholarship for carrying out this research work and providing me with some relevant literature to carry out the work.

I would like to thank Mr. Irfan Awan for providing me the support and helping me out to get through the darkest hours while working with Matlab.

I would also like to pay my sincere gratitude to Sven-J*ö*ran Schrader for his supervision and guidence during my summer job at NSB.

June 10, 2015

Muhammad Umer Nawaz

Abstract

The research is initiated with the aim to make the tunnel resistance estimations more accurate. Tunnel resistance is measured to calculate running times and energy consumption. From previous studies performed by Norges Statsbaner-NSB, it is found that the standard methods in Open Track and Viriato 6 simulation tools, used to measure tunnel resistance overestimate its value which leads to higher estimation of running times and energy consumption. But in reality, train experiences less resistance while crossing the tunnels. With the purpose to measure tunnel resistance more accurately, an attempt is made to develop new methodology that can eliminate the overestimation of tunnel resistance thus making the railway system more efficient.

In order to establish the methodology of calculating tunnel resistance, train resistance, its types and extent to which these resistances effect train motion inside tunnels are investigated. Running resistance value changes significantly inside the tunnels mainly because of change in aerodynamics. Running resistance depends on three coefficients A, B and C and among these three coefficients, C shows more variations as it depends on aerodynamics inside the tunnel. Therefore, efforts have been made out to measure the new value of coefficient C and tunnel factor is estimated using the new value of this coefficient C. Data for the research work was gathered both from NSB and Stadler. NSB conducted the test runs on NSB Type 73 and 75 while Stadler performed the test runs only on Type 75. On the basis of available data sets, direct and velocity fitting approaches are developed for tunnel resistance calculations.

Direct and velocity fitting approaches are compared with each other and also with standard Open Track and Viriato 6 methods based on tunnel factors. Results show that both the methods provide lower tunnel factors than standard values used in Open Track and Viriato 6 thus eliminating the overestimation problem. It is also found from the results that the velocity fitting method has less variations in tunnel factors for same tunnel type and provides better estimation of tunnel resistance than direct method. Therefore, tunnel factors are calculated using velocity fitting approach based on tunnel types and it ranges from 4.1 to 7.7 kg/m. Based on the results, it is suggested to use 7.7 kg/m for single track tunnels with small cross-section, 6.4 kg/m for double track tunnels with small cross-section and 4.1 kg/m for double track tunnels with large cross-section to calculate the tunnel resistance more accurately.

List of Abbreviations

ASR	Asker
BVO	Bjørkevoll
D	Direct Approach
DRM	Drammen
EV	Eidsvoll
EVV	Eidsvoll Verk
GAR	Gardermoen
JBV	Jernbaneverket
KRS	Kristiansand
LIE	Lier
LLS	Lillestrøm
LYS	Lysaker
MOI	Moi
NSB	Norges Statsbaner
OSL S	Oslo Senter
OT	Open Track
SIR	Sira
SKØ	Skøyen
SNA	Snartemo
SNCF	Société Nationale des Chemins de fer Français (French National Railways)
STO	Storekvina
SV	Sandvika
SVG	Stavanger
TEE	Trans Europe Express
VF	Velocity Fitting Approach

List of Symbols

η	Traction coefficient
ι	Longitudinal Gradient
ρ	Mass Factor
$\sum_l$	Tunnel cross-sectional area
C	Total resistance coefficient depends on aerodynamics
C_o	Open air resistance coefficient
E_{in}	Energy into the train
E_{netto}	Net energy consumption
E_{rekup}	Regenerated energy
F_{net}	Net force on train
F_{tr}	Traction force
F_{tr}^{max}	Maximum traction force
F_g	Gradient force
k_1	Constant depends on shape of nose and tail of train
k_2	Constant depends on condition of train surface
f_T	Tunnel factor
M_{rot}	Rotating mass of train
P_{aux}	Auxilliary power
P_{net}	Net power
P_{net}^{max}	Maximum net power
P_{tot}	Total power
P_{tr}	Tractive power
q	Mass coefficient
R	Radius of curvature
R_c	Curve resistance
r_c	Specific curve resistance
R_g	Gradient resistance
r_g	Specific gradient resistance
r_{in}	Specific inertial resistance
$R_{inertia}$	Inertia resistance
R_L	Running resistance
R_o	Open air resistance
R_t	Tunnel resistance
R_{tot}	Total train resistance
t_{avg}	Average cycle time

t_{max}	Maximum cycle time
v_{calc}	Calculated velocity
v_{max}	Maximum velocity of train
A	Mass dependent resistance coefficient
B	Resistance coefficient that depends partly on mass and partly on velocity
L	Length of train
M	Total train mass
N	Number of raised pantographs
p	Partial perimeter of rolling stock down down to rail level
P	Total train mass
S	Front surface cross-sectional train area
v	Velocity of train

Table of Contents

List of Figures

List of Tables

1. Introduction

This chapter describes the background of this research work followed by the problem formulation, research questions and objectives. Different software used for numerical integration and data representation are mentioned followed by the limitations and report outline. Report outline tells about the sequence in which the work is carried out to achieve thesis objectives.

1.1 Background

Running resistance of train directly effects journey times and energy consumption and it is therefore important to estimate these values as close to real value as possible. It will help in making better estimations of journey times and energy consumption and will benefit in making the punctuality better.

Norwegian Ministry of Transport and Communications is interested in making the transport system easier, faster and more modern. In the National Transport Plan of 2014-2033, budget put aside for the development of railway sector is almost double than it is given in the plan 2010-2013[9]. Increase in the speed of trains in railway sector raises a discussion of other problems. Of these, running resistance of train is of major concern. As the speed of the train increases, so does the resistance.Therefore, it is important to develop appropriate method to estimate running resistance in order to make running railway system more efficient.

Running time of a train can be calculated from infrastructure model along with a description of train's acceleration and resistance. The acceleration of a train is a well defined parameter but train resistance varies and these variations cause inaccurate estimation of running times and energy consumption. Train running under open sky experiences different resistance than the train running inside the tunnel. As it enters into the tunnel, the resistance increases signifi-

cantly and this leads to a higher energy demand as well as reduced acceleration and in some cases reduced top speed. The increase in the resistance is due to that the air is barely able to find the way to pass outside the train which leads to increased pressure variations inside the tunnel. The factors that usually influence resistance of trains are train design, tunnel length, tunnel height, tunnel profile, speed of train while entering in a tunnel, pressure variations etc. Significant research has been done to study the effects of these factors on train while running through the tunnel and standard coefficients have been estimated to calculate resistance.

1.2 Problem Statement

The tunnel resistance is becoming increasingly important with the building of new high-speed tracks, both as a result of the increased number and length of tunnels due to less flexible curvature, as well as the increased aerodynamic resistance at higher velocities. A precise estimate of the tunnel resistance is important both for the estimation of running times and energy consumption.
A tunnel confines the air flow around the train which leads to increased aerodynamic resistance. This leads to a higher energy demand as well as reduced acceleration and in some cases reduced top speed. However, NSB experiences that the standard equations for the calculation of tunnel resistance in many cases overestimate its value. This leads to too high estimates of running time and energy consumption. In order to improve these estimates, the study is initiated to get the answers of the following questions.

- Study the factors that affect the train resistance significantly inside the tunnels
- Develop the new methodology to estimate the tunnel resistance

1.3 Objectives

Main objectives of the thesis are:

1. Develop the new methodology to estimate the tunnel resistance.
2. Estimate the tunnel factor using available data sets.

3. Comparison of the methodologies developed for tunnel resistance calculations based on tunnel factors.

4. Suggest the method that estimates tunnel resistance more accurately.

1.4 Software

Simulations are performed by using programming language $Python$ including scientific Python libraries; $Numpy$ and $Scipy$. Another simulation tool named as $OpenTrack$ is used to compare the test run results with the modelled run results to figure out the sections where data sets show irregularities. $Matlab$ is mainly used for represention of extracted results from Python.

1.5 Limitations

- Resistance due to curve radius is disregarded.
- Adhesion factor is not taken into account.

1.6 Structure of the Report

Chapter 2 illustrates the train resistance, its types, highlights the running resistance as a main parameter that changes significantly inside the tunnels, represents the equations developed to estimate it and the reasons to change running resistance in tunnels.
Chapter 3 provides the details about the available data used to estimate the tunnel resistance.
Chapter 4 consists of methods developed for running resistance calcualtions based on the availability of data.
Chapter 5 represents the results obtained after performing calculations using methods mentioned in Chapter 4 and provides the discussion about the results obtained.
Chapter 6 wraps up the thesis work followed by the suggestions for future work.
Figure 1.1 represents the approach in steps to achieve the desired objectives.

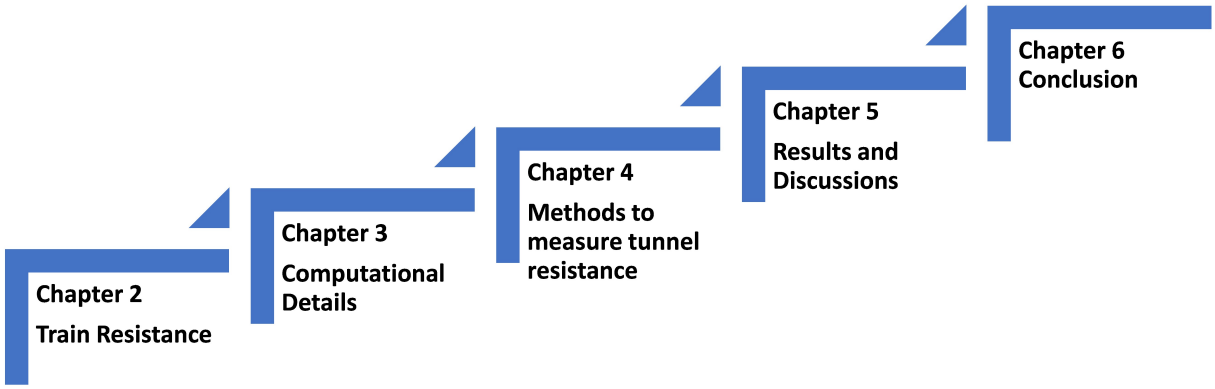

Figure 1.1: Report structure

2. Train Resistance

In this section, different types of resistance are demonstrated along with their contributions in estimation of overall train resistance. The Profillidis equation is then mentioned to measure running resistance and equations to evaluate resistance coefficients are mentioned. Further, the key factors that cause increase in the running resistance in tunnels are illustrated.

2.1 Types of Train Resistance

For the better estimation of journey times and energy consumption, forces acting in a direction opposite to the train motion need to be measured more accurately. These forces known as the resistance forces effect the top speed and accelerating ability of train [10].
According to Profillidis, the total train resistance is the sum of curve resistance, inertia resistance, gradient resistance and running resistance as shown in Equation 2.1 [14].

$$R_{\text{tot}} = R_{\text{c}} + R_{\text{inertia}} + R_{\text{g}} + R_{\text{L}} \tag{2.1}$$

where

R_{tot} = Total train resistance

R_{c} = Resistance due to curve in tracks

R_{inertia} = Resistance due to inertia

R_{g} = Resistance due to gradient

R_{L} = Running resistance

2.1.1 Curve Resistance

Resistance arising due to curves in tracks is known as curve resistance. When a train passes through a curved path, extra effort is required to overcome the resistance. There are few reasons behind increase in resistance [6].

- It arises because of rigidness of wheel. As a train moves along the curve, its frame takes up a tangential position. Because of it, flange of the outer wheel of leading axle rubs against inner surface of rail and increases the resistance as shown in Figure 2.1.

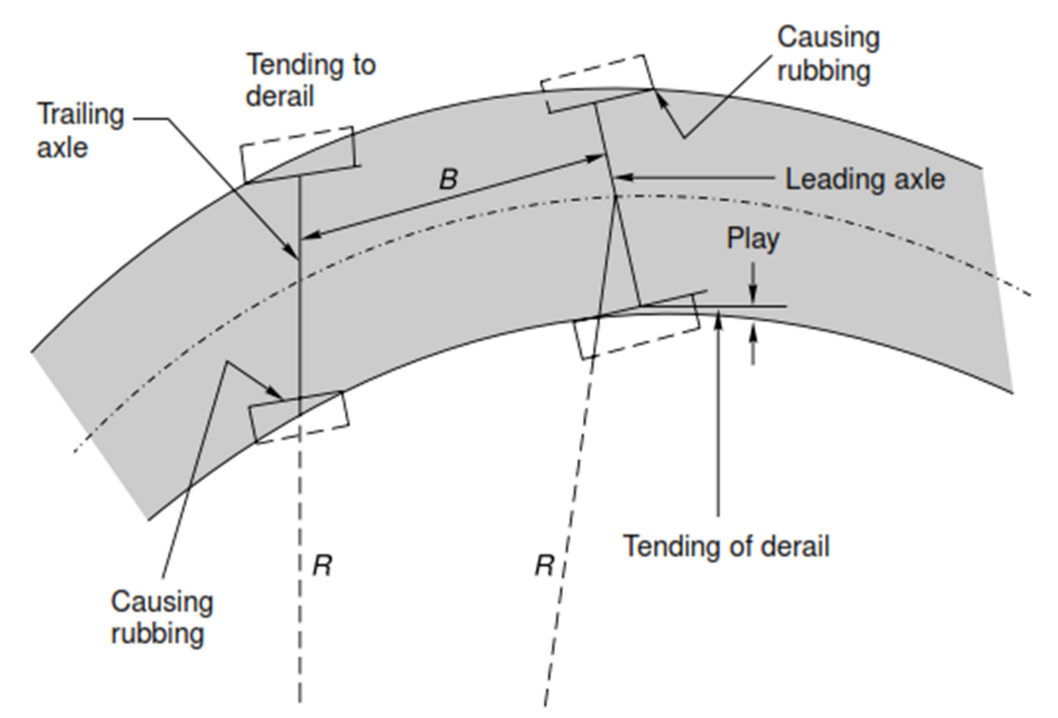

Figure 2.1: Resistance due to curve[6]

- Slippage of wheel on the rail also increases its resistance. It occurs when outer wheel flange of trailing axle remains clear and tends to derail. It can turn out worse where the curve radius is small.

- Poor maintenance of track also increases the train resistance. Improper maintenance includes worn out rails, bad alignment of tracks and lack of balancing.

- Cant of a railway also known as superelevation is another factor behind increase in resistance. Inadequate superelevation results in excessive pressure on the outer rail and excess superelevation transfers more pressure on the inner rails which results in excessive resistance.

Specific curve resistance can be estimated by using equation 2.2[14].

$$r_c = \frac{k}{R} \tag{2.2}$$

where k is a parameter with the values between 500 and 1200 and R is the radius of horizontal plane curvature.

2.1.2 Inertia Resistance

It is the resistance produced during train acceleration and is proportional to train mass and acceleration. Specific inertial resistance is estimated by using equation 2.3 [14].

$$r_{in} = (\frac{\alpha}{g})q \tag{2.3}$$

where r_{in} is the inertial specific resistance, α is the acceleration imparted by the traction engine, q is the mass coefficient and g is the gravitational acceleration. q takes into account both fixed and rotational masses of the vehicle and is expressed in equation 2.4 [14]:

$$q = 1 + \frac{M_{rot}}{M} \tag{2.4}$$

where M_{rot} is the rotating mass of the vehicle. The rotating mass is derived from the rotational inertia and the angular velocity of the shafts, motors, transmissions etc. while M is the total mass of the train.

2.1.3 Gradient Resistance

Along a straight level track, value of gradient resistance is zero because the force component perpendicular to the direction of gravity is zero. The gradient force contributes in train resis-

tance when the track in inclined as shown in Figure 2.5. It increases the resistance only when the train moves upward[14] and reduces the resistance when the train goes downward.

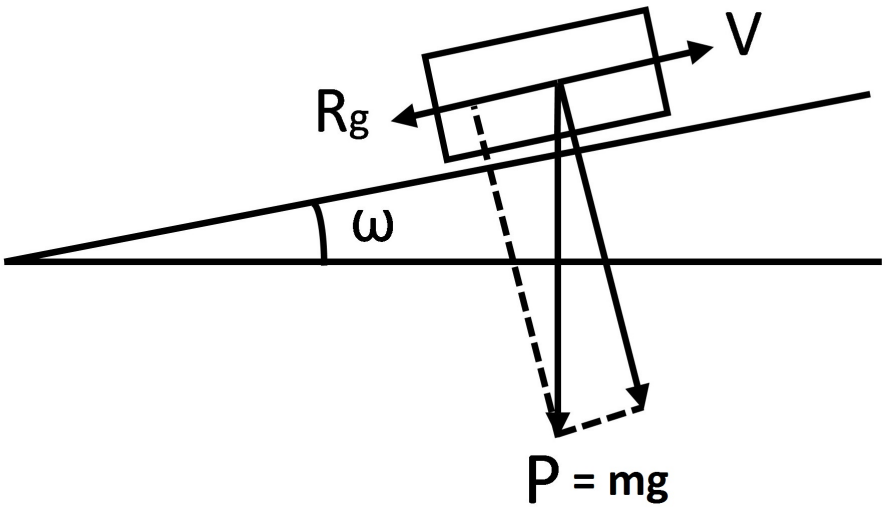

Figure 2.2: Gradient resistance[14]

It can be calculated by using the equation 2.5 [14].

$$R_g = m.g.sin\omega \tag{2.5}$$

where

m = mass of the train

g = acceleration due to gravity

ω = angle of inclination

Because of the small angle of gradient, $sin\omega$ can be written as:

$$sin\omega \approx tan\omega = \iota \tag{2.6}$$

where ι is the longitudinal gradient and its value is usually given in permil. Equation 2.7[5] shows modified form of gradient formula.

$$R_g = m.g.\iota \tag{2.7}$$

In absolute form, gradient resistance depends on train weight and it is not practical to repre-

sent it in terms of weight. Instead of representing in absolute form, grade resistance is usually represented in specific form. Equation 2.8 [13] illustrates the specific grade resistance formula.

$$r_{\text{grade}} = \frac{R_{\text{grade}}}{m.g} = sin\alpha \approx tan\alpha = \iota \tag{2.8}$$

where r_{grade} is the specific resistance or effort and is measured in N/kN or permil (‰).

$$1N/kN = 1/1000 = 1permil \tag{2.9}$$

In equation 2.8, sine angle is replaced by the tangent because of relatively small value of gradient angle and is equal to ι known as grade quotient.

2.1.4 Running Resistance

Formula to approximate running resistance of train was developed by Strahl in 1913 and by Davis in 1926 [11]. Equation 2.10 [14] represents the formula proposed by the Davis for running resistance estimation.

$$R_{\text{L}} = A + BV + CV^2 \tag{2.10}$$

First two terms $A + BV$ represent mechanical resistances. The first term A is independent of speed and only depends on vehicle characteristics. It represents the rolling and friction resistances between wheel flange and rail on curves. The term BV is partly velocity dependent and partly mass dependent and represents resistances because of axles and shafts rotation, mechanical transmission and braking etc. The last term CV^2 depends only on train speed and represents aerodynamic drag [14].

Among all types of train resistance, running resistance changes significantly when the train enters into the tunnel. It is because it depends on the aerodynamics of train. Aerodynamics changes abruptly inside the tunnels and are illustrated in section 2.3.2.

2.2 Running Resistance Coefficients

A numer of test runs have been performed and methods have been developed to estimate the train running resistance [11][20]. Different values of train resistance coefficients are obtained with different methods but have small deviations. The equations used by Profillidis and French Railway Authority to estimate these coefficients are presented here.

2.2.1 Profillidis Resistance Coefficient Equations

Profillidis developed equations to estimate coefficients A, B and C and these coefficients depend on the vehicle characteristics. Values of the coefficients vary from vehile to vehicle depending on total mass, mass per axle, length, front surface cross-section area etc.

$$A(kg) = \lambda M\sqrt{\frac{10}{m}} \tag{2.11}$$

In equation 2.11 [14], M (tons) is total mass of the train, m (tons) is mass per axle and λ is the parameter with values depending on vehicle type.
For French National Railways (SNCF) vehicles, value ranges from $0.9 < \lambda < 1.5$ [14].

$$B.V(kg) = 0.01MV \tag{2.12}$$

In equation 2.12 [14], M (tons) is the mass of the train and V (km/h) is the velocity of the train. This equation is valid for good quality track and rolling stock on bogies.

$$CV^2(kg) = k_1SV^2 + k_2pLV^2 \tag{2.13}$$

Equation 2.13 [14] demonstrates the aerodynamic drag on trains. The first term (k_1SV^2) of the equation represents the aerodynamic drag arises at the nose and the tail of the train and the next term (k_2pLV^2) of the equation illustrates the aerodynamic drag generated along the surface[14]. where

k_1 = Parameter depends on the shape of the nose and the tail of train

S = Front surface cross sectional area $[m^2]$

k_2 = Parameter depends on the condition of the surface

p = Partial perimeter of the rolling stock down to rail level [m]

L = Train length [m]

V = Velocity of train [km/h]

2.2.2 French Railway Authority Resistance Coefficient Equations

Equations used to estimate the running resistance coefficients by French Railway Authority for electric commuter trains are represented in equations 2.14, 2.15 and 2.16 [14].

$$A(kg) = 1.3\sqrt{\frac{10}{m}}P \tag{2.14}$$

$$B(kgs/m) = 0.01P \tag{2.15}$$

$$C(kgs^2/m^2) = 0.0035S + 0.00041\frac{\rho L}{100} + 0.002N \tag{2.16}$$

where

P = Total mass of the train [tons]

m = Mass per axle [tons]

V = Speed [km/h]

N = Number of raised pantographs

S = Front surface cross sectional area [m^2]

p = Partial perimeter of the rolling stock down to rail level [m]

L= Train length [m]

2.3 Train Resistance in Tunnels

The aerodynamics of a train change significantly as it enters into the tunnel. There are four main factors to consider [14].

- Pressure effects

- Increased aerodynamic resistance in tunnels
- Crossing of trains
- Tunnel cross-section

When train enters into the tunnel, changes in aerodynamics and pressure occur and it makes the running resistance calculations more complex.

2.3.1 Pressure Effects

The problem arises when the pressure fluctuates inside the tunnel. When the train passes through the tunnel, train head compresses the air in front of it and generates overpressure waves. As the train proceeds, it compresses more air and thus increasing the amplitude of overpressure wave. Overpressure wave reaches to maximum value when the train tail enters into the tunnel. As the train moves forward and compresses more air in front of it, vaccuum is generated. Because of this, underpressure waves are also generated inside tunnel as shown in Figure 2.3. The overpressure wave at the train front hits the walls of the tunnel and returns back in the form of underpressure wave. With respect to underpressure wave generated by train tail, it undergoes few changes and turns out into overpressure wave. These waves together cause pressure fluctuations in the tunnel [16].

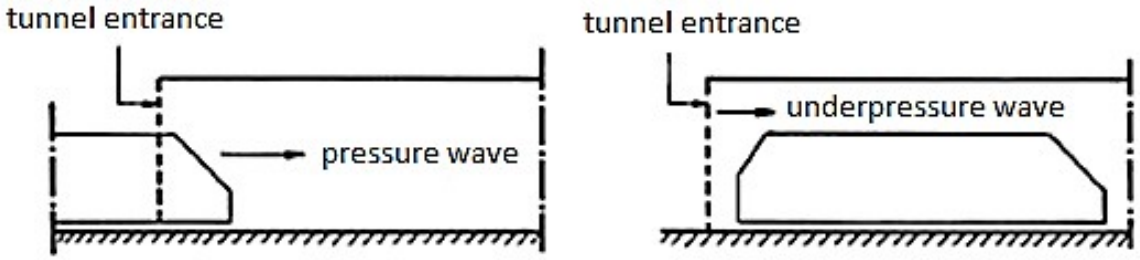

Figure 2.3: Pressure and underpressure waves when train enters a tunnel [14]

In addition to increase in resistance, pressure fluctuations might become a cause of passenger discomfort depending on the rate of change in pressure. Higher rate of change in pressure do not create discomfort to passengers, however smaller changes in rate of pressure can cause discomfort.

According to Vardy [19], as the train enters into the tunnel, it displaces the air. Some of it flows alongside the train and some moves out of the portal, but the remainder passes down the tunnel behind a pressure wavefront. As the train proceeds in the tunnel, it raises the pressure of the air in front of it as shown in Figure 2.4 which can sometimes increase by 2 kPa or more [19]. This rise in air pressure causes increase in the aerodynamic drag on train. Furthermore, pressure waves are generated when the train nose leaves the tunnel, tail enters and leaves the tunnel and when the tail and the nose pass alongside air shafts and cross passages. Figure 2.4 shows that initially pressure change is small but when once the train tail enters inside the tunnel, it increases abruptly and then starts decreasing [19].

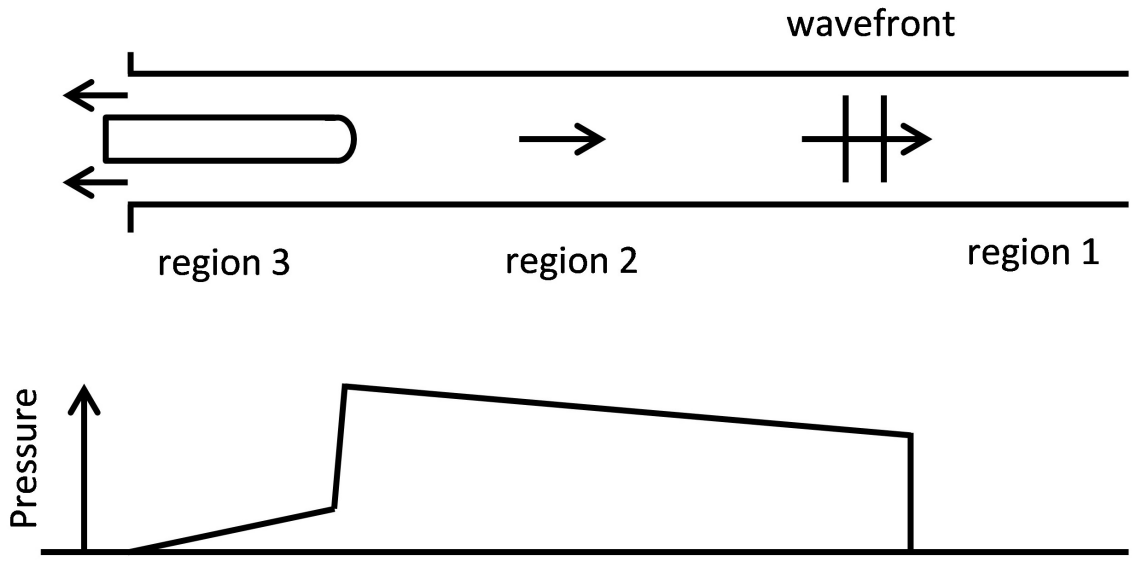

Figure 2.4: Pressure distribution during train entry[19]

2.3.2 Aerodynamic Drag

Aerodynamics play a significant role in increasing or decreasing the train resistance. In tunnels because of confined space, aerodynamics change and increases the aerodynamic drag. Significant research has already been done to overcome this problem and to reduce aerodynamic effects as much as possible. Swiss and French Railways have done research on type TEE (Trans Europe Express) rolling stock and relate the running resistance as a function of lateral openings

in the tunnel to reduce aerodynamic resistance [14]. Magnitude of change in aerodynamics depends on the tunnel cross-section and on train nose and tail shape. It can be reduced by making changes either in train shape or in tunnels cross-section. To reduce the aerodynamic drag, it is suggested to reduce the $S/\sum_l$ ratio [14].

where

S = Front surface cross-sectional train area

$\sum_l$ = Effective tunnel cross-sectional area

The proposed ratio for single track and double track tunnels are [14]:

For single track tunnels, $S/\sum_l = 0.30/0.50$

For double track tunnels, $S/\sum_l \sim 0.15$

To reduce this ratio, effective tunnel cross-sectional area needs to be increased which would lead to higher cost of tunnel construction. Another approach to reduce the aerodynamic resistance in tunnels is by reducing the pressure difference between the head and the tail of the train. This has been done in the Channel Tunnel [8], composed of two single track tunnels with communication openings every 375 m [14].

2.3.3 Train Crossing in Tunnels

As the two trains cross each other inside a tunnel, it generates pressure waves. Both exert stress on each other and the one with the higher speed produces stronger waves and the other moving at low speed bears heavy stress. But it does not cause any passenger discomfort and changes in resistance calculations because of very short passing time interval. However tests have shown that this is valid for the speed limit up to 220 km/h but beyond this limit, effects would be considerable [14].

2.3.4 Tunnel Cross-section

Tunnels cross-sections are directly related to the speed of trains. For high speed trains, tunnels should have large cross-sectional area as compared to the tunnels for low speed trains. If the speed of the train is less than 200 km/h, then the emphasis remains only on the tunnel cross-section and the distance between the tracks. If the train speed is greater than 200 km/h, then

emphasis should also be put on the performance and mechanical resistances of the rolling stock along with the cross-section and track distance. Tunnels cross-section at certain velocities are suggested by Profillidis and are displayed in Table 2.1.[14]

Table 2.1: Tunnel cross-section area for double track tunnel at various speeds [14]

$V_{max}(km/h)$	160	200	240	300
$\sum_l(m^2)$	40	55	71	100

2.4 Traction Force

The force at the driving wheels of a train that starts and moves tonnage up various elevations. It depends on the adhesion of wheels on the rails and the maximum value of traction force can be estimated by the product of weight on driving wheels and coefficient of adhesion[15]. When the train is at rest, the traction force will be the highest and as the speed of the train increases the traction force starts decreasing. Adhesion limits the value of traction force and because of it, traction force cannot be increased beyond a certain level.

3. Computational Details

The data used to estimate the tunnel resistance is collected from Open Track, Banedata, Jernbaneverket and test runs conducted by NSB and Stadler. Data inside the tunnels is only used for measuring tunnel resistance. Mainly the data is extracted from run down tests performed by NSB and Stadler. NSB performed the test runs between Drammen and Eidsvoll and from Stavanger to Kristiansand on two different locomotives named as NSB Type 73 and Type 75[1] but Stadler conducted test runs only between Drammen and Eidsvoll. Details of the tunnels along with their lengths and directions are shown in Tables 3.1 and 3.2.

Table 3.1: Tunnels details between Drammen and Eidsvoll[3]

Tunnel Name	**Direction DRM to EV**	**Direction EV to DRM**	**Tunnel Length [km]**
Romeriksporten	OSL S to LLS	LLS to OSL S	14.574
Bærumstunnelen	SV to LYS	LYS to SV	5.446
Tanumtunnelen	ASR to SV	SV to ASR	3.492
Skaugumtunnelen	ASR to SV	SV to ASR	3.790
Lieråsentunnelen	LIE to ASR	ASR to LIE	10.723

Table 3.2: Tunnel details Stavanger to Kristiansand [3]

Tunnel	**Stavanger to Kristiansand**	**Tunnel Length [km]**
Kvineshei	STO to SNA	9.065
Siratunnelen	SIR to BVO	3.107
Tronåstunnelen	MOI to SIR	3.178

Five tunnels situated between Drammen and Eidsvoll and three tunnels situated between Stavanger and Kristiansand are used for estimating tunnel resistance. Romeriksporten is situated in between OSL S and LLS and is the longest among five tunnels with length of 14.574 km[3]. The smallest tunnel is Tanumtunnelen and is situated in between ASR and SV and its length is 3.492 km[3]. From Stavanger to Kristiansand, the longest tunnel is Kvineshei situated between STO to SNA and the smallest tunnel is Siratunnelen situated between SIR to BVO with lengths of 9.065 km and 3.107 km respectively.

3.1 Teloc Data

NSB conducted test runs on two different locomotives using Teloc 2000 and 2500. From Stavanger to Kristiansand, these runs were performed on NSB Type 73 and Teloc 2000 is used to record data. Between Drammen and Eidsvoll, these runs were performed on NSB Type 75 using Teloc 2500. For Type 73, Teloc data consists of time, distance, velocity and acceleration. For Type 75, Teloc data consists of date, time and velocity. Tables 3.3 and 3.4 display the cycle times and max velocities for both data sets.

Table 3.3: Teloc 2500 data

Tunnel Names	**Direction DRM to EV**			**Direction EV to DRM**		
	V_{max}	**Cycle Time [sec]**		V_{max}	**Cycle Time [sec]**	
	[km/h]	t_{max}	t_{avg}	**[km/h]**	t_{max}	t_{avg}
Romeriksporten	200.54	16.98	0.52	200.081	12.56	0.47
Bærumstunnelen	159.373	13.78	0.38	157.88	17.12	0.40
Tanumtunnelen	159.949	5.26	0.40	160.75	15.6	0.48
Skaugumtunnelen	159.949	5.26	0.40	160.75	15.6	0.48
Lieråsentunnelen	129.39	27.67	0.51	128.9	10.16	0.87

For Type 75, these runs are compared with the modelled runs from Open Track (OT). Curves are drawn by extracting data from Open Track and Teloc and show deviations at some sections.

Table 3.4: Teloc 2000 data

Tunnel	V_{max} [km/h]	Cycle Time [s]	
		t_{max}	t_{avg}
Kvineshei	160.61	66.30	7.00
Siratunnelen	120.97	70.90	11.99
Tronåstunnelen	129.39	23.90	4.95

These deviations observed are mainly because of early braking by the driver, poor adhesion at certain areas on the tracks and bad weather conditions. Because of these practical issues, the results at these sections were unexpected when are compared with the results from Open Track. Figures 3.1, 3.2 and 3.3 demonstrate the areas where deviations occur berween the modelled and the test runs.

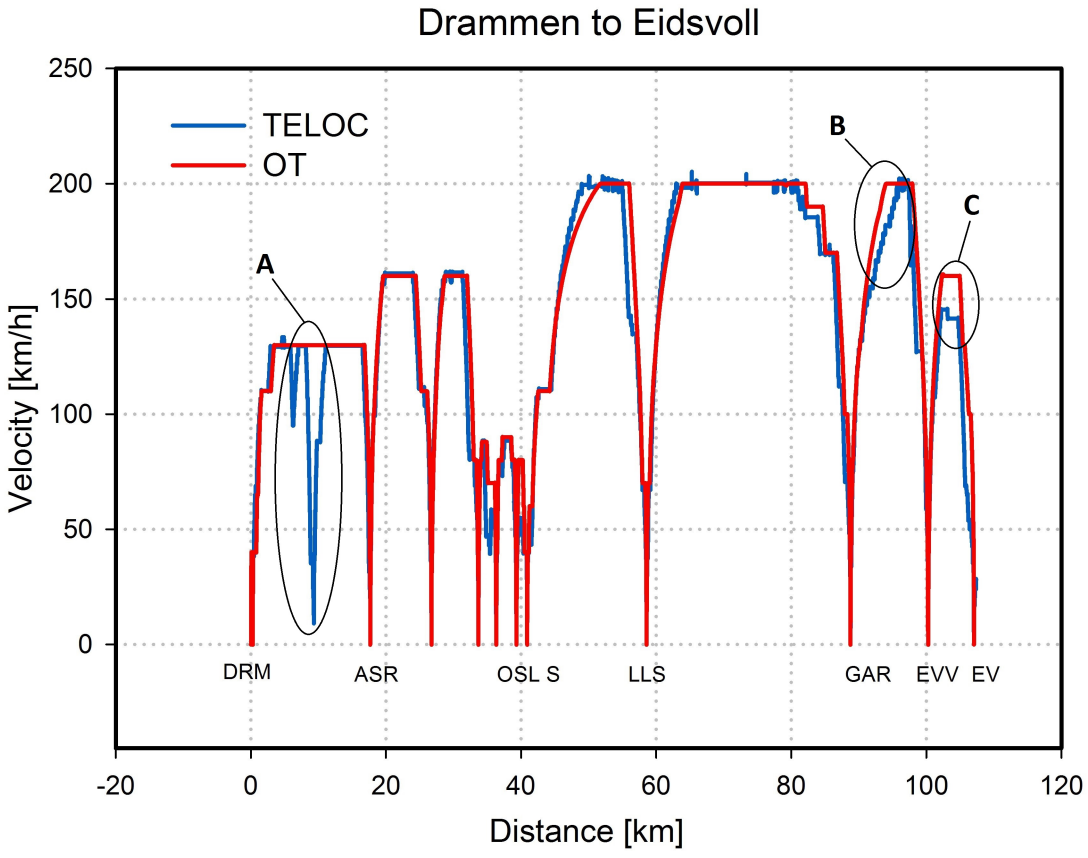

Figure 3.1: Differences between Open Track and Teloc curves from DRM to EV

Blue curves are plotted using Teloc data and red curves are plotted by extracting data from Open Track. Major deviations in graphs are marked as A, B, C and D. Figure 3.1 blue curve deviates from the red curve mainly at three points. In the area A while heading towards Asker, Teloc curve

suddenly drops down on the middle of its way to Asker but then increases again and achieves required speed limit. This happened because of signal failure. The train came across red signal on its way to Asker and the driver had to reduce the train speed.

In area B while running from Gardermoen to Eidsvoll verk, the red curve lags behind the blue curve while approaching maximum speed limit. This happened because of the poor adhesion between the rail and wheels of the train caused by bad weather conditions. In area C while travelling from Eidsvoll verk to Eidsvoll, the maximum speed limit allowed is 160 km/h but the driver intentionally drove at 140 km/h.

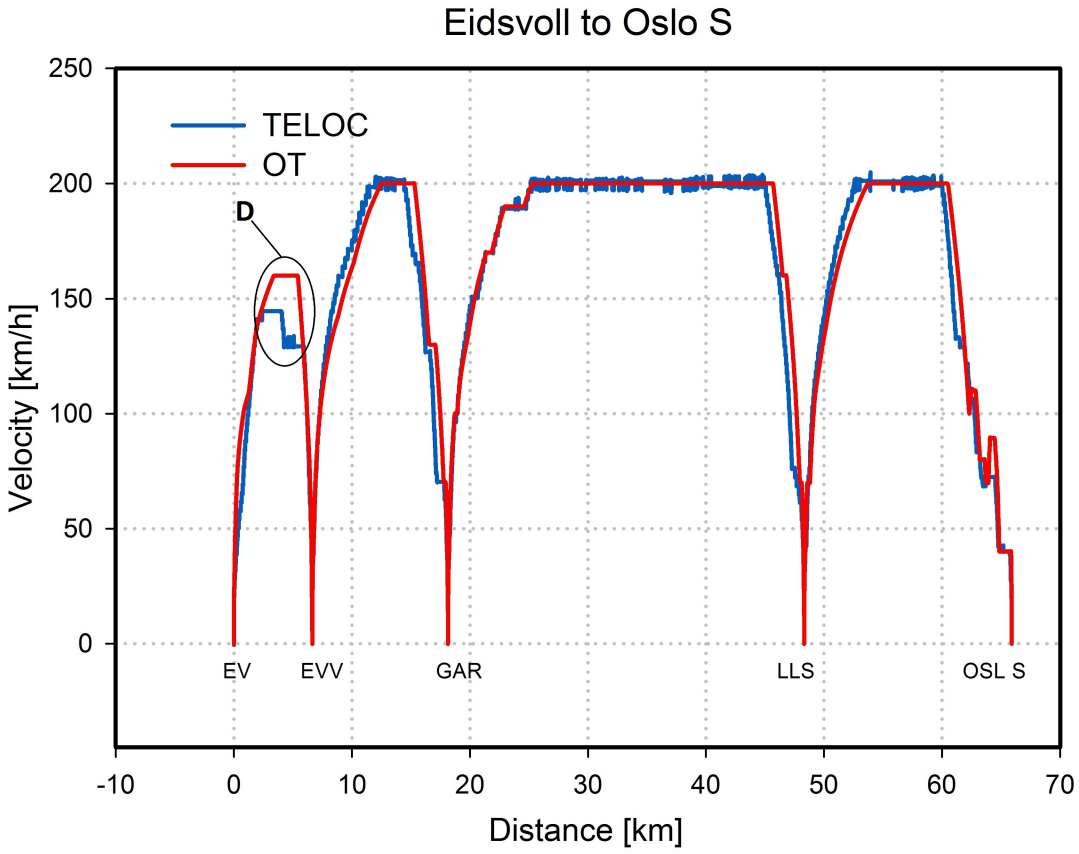

Figure 3.2: Differences between Open Track and Teloc curves from EV to OSL S

Figures 3.2 and 3.3 illustrate the Teloc and Open track curves from Eidsvoll to Drammen. In this data set, deviations are quite lower as compared to the previous test run from Drammen to Eidsvoll. Figure 3.2 displays major deviation at only one point marked as area D. While travelling from Eidsvoll to Eidsvoll verk, the driver drove at lower speed than maximum allowed speed. In Figure 3.3, the Teloc curve matches well with the Open Track curve and does not have any major

deviation throughout the run.

Figures show that during deceleration, Teloc curves usually lag behind the Open track curves and it is because of the early braking applied by the driver. The major differences between Teloc and Open Track curves exist because of the above mentioned irregularities and incidences occurred on the day when the test runs were performed.

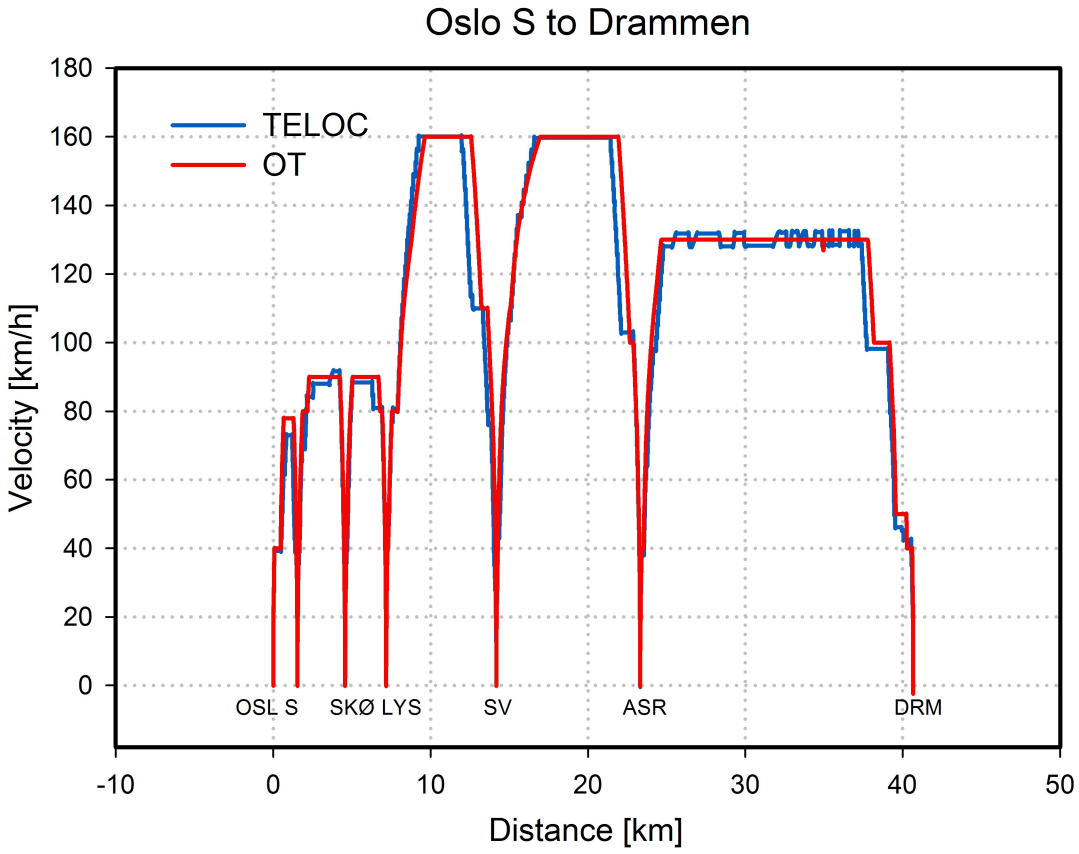

Figure 3.3: Differences between Open Track and Teloc curves from OSL S to DRM

3.2 Energy Data

Another approach of measuring tunnel resistance of train is by using energy data. Estimated value of tunnel resistance will then be compared with the value estimated by Teloc data. This data set is recorded by Stadler while performing the test runs before handing over the new Type 75 to NSB. This data set consists of date, time, velocity and three types of energy values which are E_{in} (energy into the train), E_{rekup} (regenerated energy) and E_{netto} (net energy consumption).

Table 3.5: Energy data between DRM and EV

Tunnels	Direction DRM to EV		Direction EV to DRM	
	V_{max} [km/h]	Cycle Time [s]	V_{max} [km/h]	Cycle Time [s]
Romeriksporten	163	0.2	165	0.2
Bærumstunnelen	107	0.2	96	0.2
Tanumtunnelen	164	0.2	162	0.2
Skaugumtunnelen	164	0.2	162	0.2
Lieråsentunnelen	132	0.2	35	0.2

3.3 Gradients

Gradient values play important role in estimation of tunnel resistance. These are taken from Banedata and are given in the form of step functions with constant value sections as shown in Tables 3.6 and 3.7.

Table 3.6: Gradient values for tunnels between DRM and EV

Tunnel Names	Direction DRM to EV		Direction EV to DRM	
	Gradient Values [permil]			
	max	**min**	**max**	**min**
Romeriksporten	6.71	-12.23	12.23	-6.71
Bærumstunnelen	12.27	-15.54	15.54	-12.27
Tanumtunnelen	11.78	-13.09	13.09	-11.78
Skaugumtunnelen	0	-13.09	13.09	0
Lieråsentunnelen	9	-3.79	3.79	-9

The gradient values for above mentioned ten tunnels vary between 22.01 and -15.54. Positive values represent the slope as uphill and negative values represent slope as downhill. Figures 3.4, 3.5, 3.6 and 3.7 illustrate the change in the gradient and velocity along with the distance for the tunnels situated between Drammen and Eidsvoll and 3.8 shows the change in gradient and velocity for tunnels situated between Stavanger and Kristiansand.

Between Drammen and Eidsvoll, velocity and gradient curves drawn are for Teloc data. In

Table 3.7: Gradient values for tunnels between SVG to KRS

Tunnel	Gradient Values [permil]	
	max	min
Kvineshei	11	-10.7
Siratunnelen	22.01	14.98
Tronåstunnelen	10	-4
Hægebostad	4	-11.4
Gylandtunnelen	16	-6

Romeriksporten tunnel as shown in the Figure 3.4, gradient value is positive throughout the tunnel except some portion at the end and shows that the train moves uphill inside the tunnel. As the gradient is uphill, so the resistance due to gradient force will be subtracted in this region. Similarly for Bærumstunnelen, for direction from SV to LYS, gradeint values are negative during acceleraion of train.

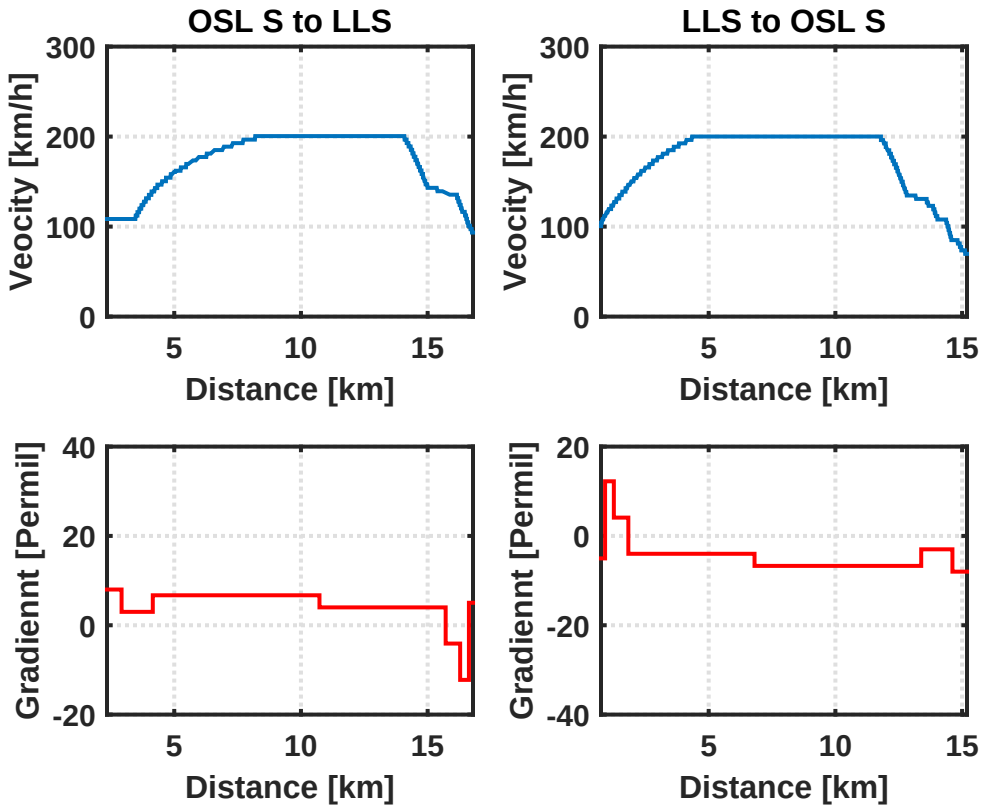

Figure 3.4: Velocity and gradient curves for Romeriksporten

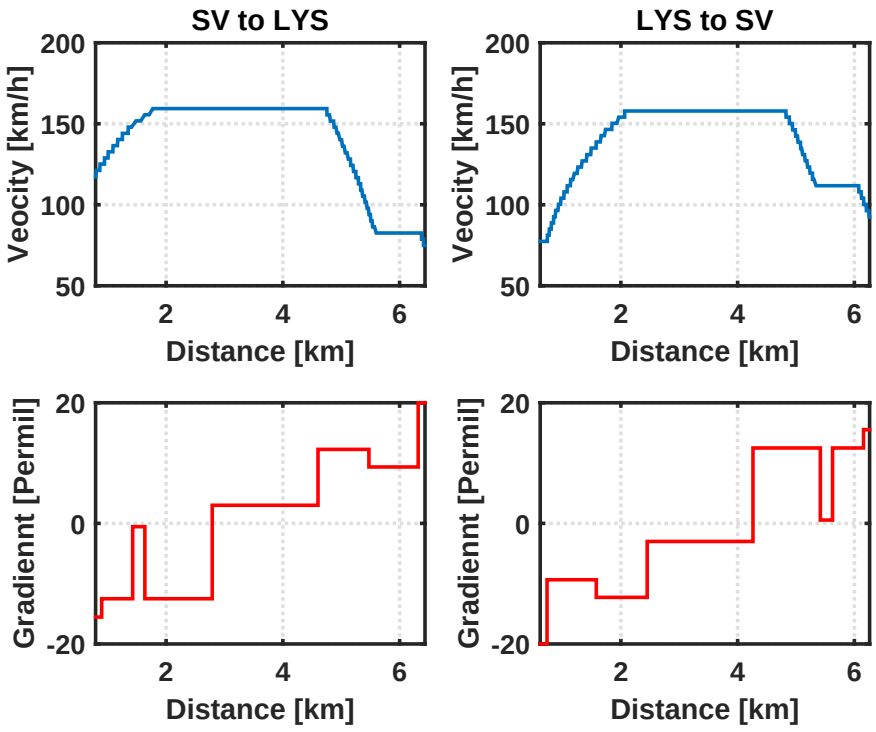

Figure 3.5: Velocity and gradient curves for Bærumstunnelen

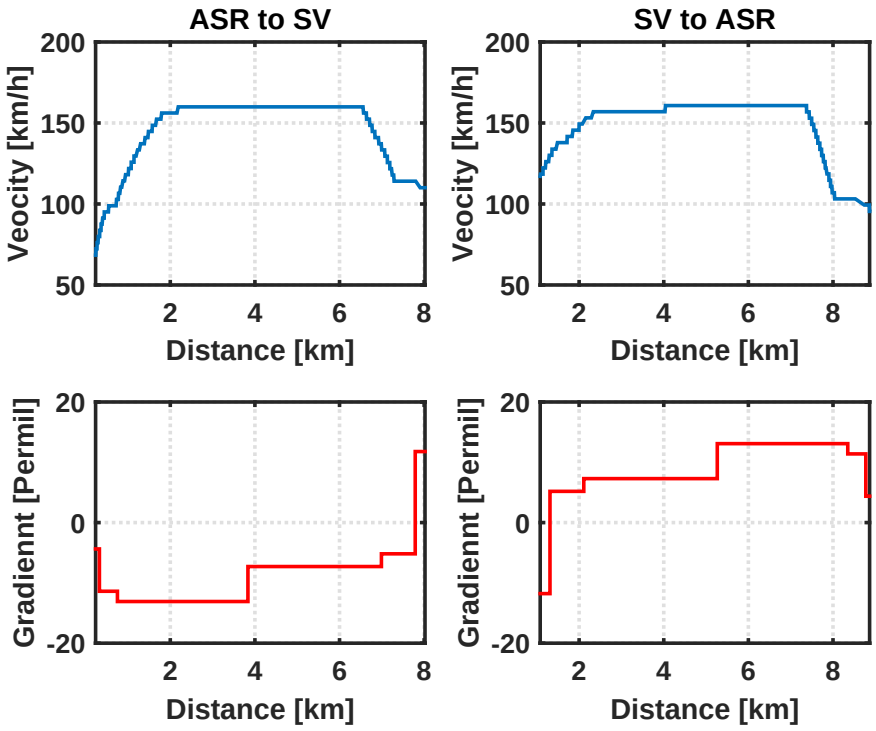

Figure 3.6: Velocity and gradient curves for Tanumtunnelen and Skaugumtunnelen

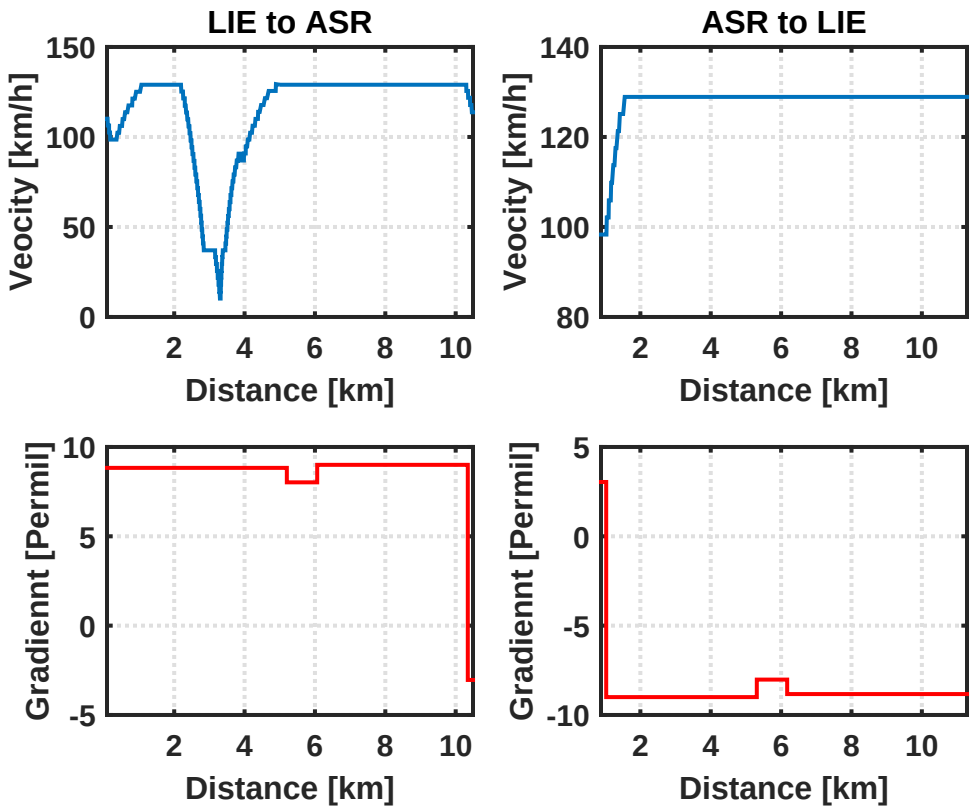

Figure 3.7: Velocity and gradient curves for Lieråsentunnelen

In Skaugumtunnelen from ASR to SV as displayed in Figure 3.6, gradient value is negative but it becomes positive when train travels from SV to ASR. In Figure 3.7 for direction from ASR to LIE, the gradient values from LIE to ASR are positive and from ASR to LIE are negative. In this tunnel, gradient value almost remains the same except some section in the middle.

Figure 3.8 illustrates change in gradient as the train proceeds further inside the tunnel. For Siratunnelen, gradient value is positive that shows that train moves uphill. For Kvineshei, half section of the tunnel has positive slope and half of it has negative slope and in Tronåstunnelen, only small section at the end has positive slope. For Gylandtunnelen and Hægebostad, gradient values are approimately positive throughout the tunnel sections except at the end for a very small section.

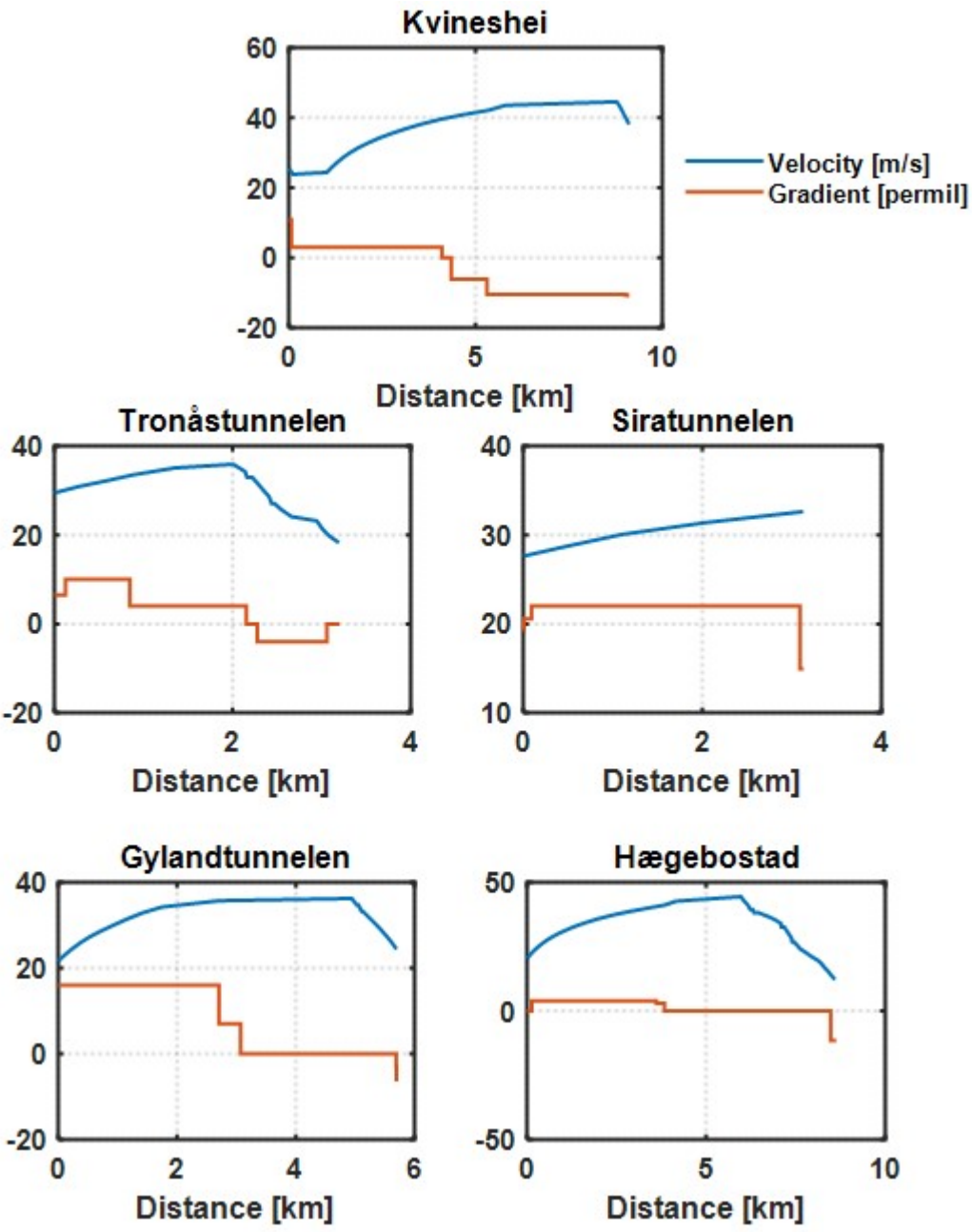

Figure 3.8: Velocity and gradient for SVG and KRS

3.4 Curve Radius

Curve radius values are step functions and are quite high for the tunnels used for measuring resistance. Therefore, these values are disregarded while performing the calculations for tunnel resistance. According to the Rochard and Schmid [17], it is not necessary to consider the

resistance due to curve if value of curve radius is greater than 250 m. Tracks from Drammen to Eidsvoll are almost straight and are shown on Jernbaneverkets Kartvisning [3].

3.5 Traction Force

Traction force used to estimate running resistance has different values both for Teloc data and for energy data. For Teloc data, traction force values used to estimate tunnel resistance are provided by Stadler for Type 75. But for energy data, it is calculated from energy values. It is described in detail in the Chapter 4.

4. Methods to Measure Tunnel Resistance

The equations and methods description used in this chapter are taken from the research paper [12] to be submitted. Two different approaches to estimate the tunnel resistance have been studied, a direct estimation using the measured or logged acceleration and an indirect estimation based on the fitting of a calculated velocity profile to the measured velocity profile, where the train resistance is implicit in the calculation of the velocity profile.

4.1 The Direct Approach

In the direct approach, a time-series of the train resistance is obtained by using a force balance and adding or subtracting terms to get the resistance. The net force acting on a train is represented by equation 4.1 [12].

$$F_{net} = F_{tr} + F_g - R_{tot} \tag{4.1}$$

Where F_{net} is the net force, F_{tr} is the traction force, F_g is the gradient force and R is the total resistance acting on the train and is defined as the force acting in the opposite direction of train motion. Equation 4.1 can be rewritten as:

$$R_{tot} = F_{tr} + F_g - F_{net} \tag{4.2}$$

To obtain R_{tot} we require the traction force, the gradient force and the net force. Assuming the train as a point mass, an expression for F_g is shown in equation 4.3 and by using Newtons's second law of motion, F_{net} is expressed in equation 4.4 [7][12].

$$F_g = -mg\sin(\alpha) = (-mg)\frac{p}{\sqrt{p^2+1}} \approx -mgp \tag{4.3}$$

$$F_{net} = m\rho a \tag{4.4}$$

$$R_{tot} = F_{tr} - mgp - m\rho a \tag{4.5}$$

Where m, a, g, p, ρ is the mass, acceleration of the train, the gravitational constant, the gradient which is defined as positive for a train running uphill and the mass factor respectively. The latter models the effect of accelerating rotational components of the train as the train itself accelerates, and is defined as the relationship between the rotational energy of the components to accelerate and the translational energy of the train. This is a common approximation [7].
The mass and mass factor of the train are assumed to be known and the gradient is a known parameter as well, the remaining unknown parameters in equation 4.5 are the traction force F_{tr} and the acceleration a. The variants of the direct approach are distinguished by different ways to obtain F_{tr} and a.

4.2 The Velocity-Fitting Approach

In the velocity-fitting approach the resistance is not monitored directly but input into the calculation of a velocity profile which is compared to the measured velocity profile. The parameters of the resistance formula are then obtained by a least-squares fit to the measured velocity profile. Equation 4.5 can be rearranged to obtain the expression for aceleration and it is shown in equation 4.6.

$$a = \frac{F_{tr} - mgp - R_{tot}}{m\rho} \tag{4.6}$$

In principle, we can obtain a calculated velocity (v_{calc}) by integrating the acceleration from a given starting time t_0 and velocity v_0 as shown in equation 4.7.

$$v_{calc}(t) = v_0 + \int_{t_0}^{t} a(t')\,dt' \tag{4.7}$$

This is the same integral as is solved in a common run-time calculation. To be able to solve

this integral an expression for R_{tot} is needed, and the resistance is commonly assumed to be a function of the velocity [5][14][17][11][7] and a set of parameters (A,B and C) and can be written as shown in equation 4.8.

$$R = A + BV + CV^2 \tag{4.8}$$

$v_{calc}(t)$ which depends on the same set of parameters in addition to v_0 can be obtained by fitting these parameters. It is done by minimizing the difference between the calculated and observed velocity and can be written as shown in equation 4.9.

$$min \qquad |v_{calc}(t; v_0, A, B, C) - v_{obs}(t)| \qquad w.r.t. \quad v_0, A, B, C \tag{4.9}$$

This approach will automatically give the resistance as a function of velocity whereas the direct approach will give a time-series of resistance values, which have to be post-processed to be expressed as a function of velocity. The variants of the fitting approach are distinguished by different ways to obtain F_{tr}.

4.3 Traction Force from Trains in Operation

In both the direct and the velocity-fitting approaches an expression for the traction force is needed. In most cases the traction force is not logged from a train in operation, however under specific circumstances the traction force may be derived during two phases.

- Maximum traction phase: The maximum traction force is in general a result of the maximum power and adhesion, and is commonly specified for a train set by the supplier. The application of maximum traction force can be ensured by instructing the driver. If maximum traction is applied, one can then use the acceleration phase for analysis. These are easy to identify and span a large velocity range.

- Coasting Phase. While coasting, the applied traction is zero by definition. To be able to use coasting phases for analysis, parts of the run must be logged or pre-defined where coasting should be performed. In operation, coasting is commonly used close to maximum speed, and only for a short amount of time, thus sampling only a small velocity range.

The maximal traction force is commonly specified from a traction diagram for a given train unit[4], and is given below in Figure 4.1.

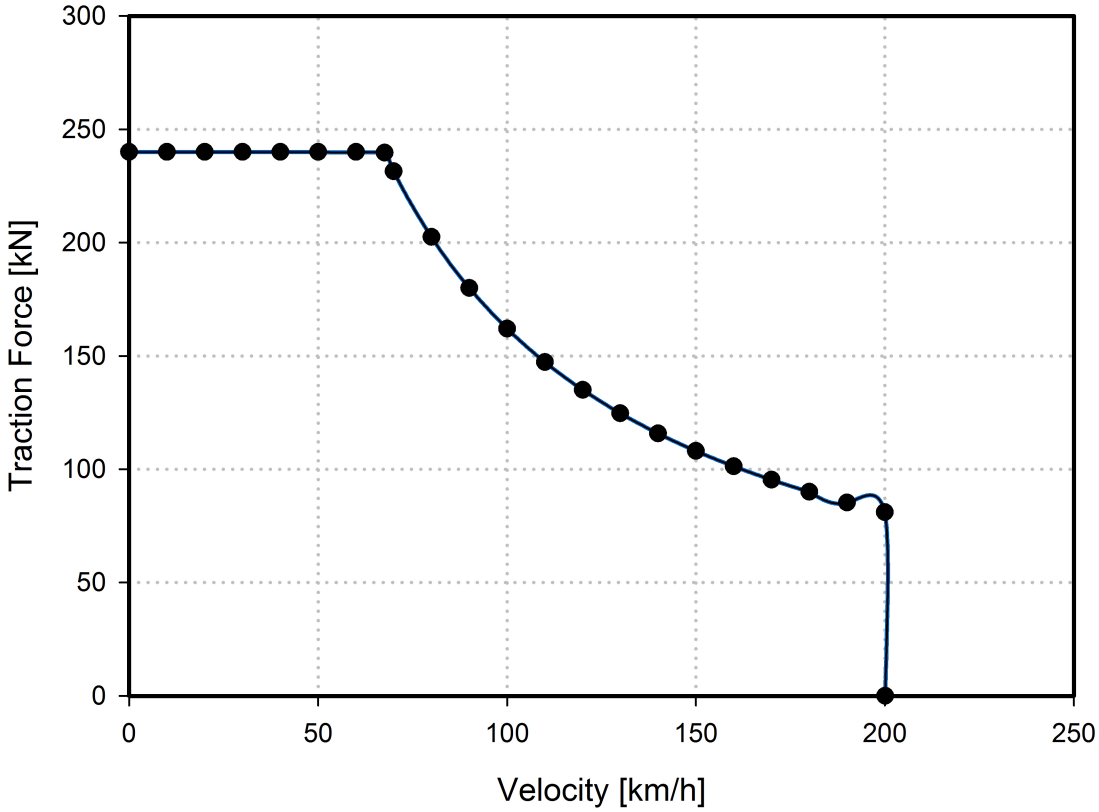

Figure 4.1: Traction force diagram [4]

This traction diagram is drawn by using the values provided by the Stadler. The black dots on the curves represent the values of traction force against certain velocities. To extract the traction force values against velocity values for running resistance estimations, interpolation is being performed. The maximum value of traction force is 240 kN at the velocity of 0 km/h. At 200 km/h, the traction force becomes 81 kN and then the slight increase in the value of velocity after 200 km/h would lead to decrease in traction force to 0 kN. According to the values provided by the Stadler, maximum traction force is 240 kN and as the speed goes beyond 200 km/h, the force reduced down to zero.

If the energy consumption of the train is logged, the power consumption P_{net} may also be derived. The power used for traction P_{tr} can then be written as shown in equation 4.10.

$$P_{tr} = P_{net} + P_{aux} \tag{4.10}$$

Where P_{aux} denotes the power consumption for auxiliary systems. Using the relation $P = Fv$ and a traction chain efficiency factor η, traction force can be estimated by using equation 4.11.

$$F_{tr} = \eta(\frac{P_{net} - P_{aux}}{v}) \tag{4.11}$$

The estimation of traction force from the energy consumption requires to know auxiliary power (P_{aux}) and the traction chain efficiency factor (η). P_{aux} can be obtained by analyzing the energy consumption during coasting phases and η can be obtained by comparing the energy consumption during a maximum traction phase and the traction force as is given in equation 4.12.

$$\eta = \frac{F_{tr}^{max} v}{(P_{net}^{max} - P_{aux})} \tag{4.12}$$

The advantage of using an estimated traction over traction force obtained during maximum acceleration and coasting phases is that no driver instruction is necessary and that the whole train run except the braking phases is available for analysis.

4.4 Decomposing the Resistance

The aim of this work is to be able to obtain a description of the tunnel resistance, which must be extracted from the total resistance. The total train resistance is commonly decomposed into contributions from open-air resistance (R_o), curve resistance (R_c) and tunnel resistance (R_t) as represented in equation 4.13.

$$R_{tot} = R_o + R_c + R_t \tag{4.13}$$

In this work, analysis of train resistance carried out in tunnels is mainly dominated by straight sections or sections with low curvature, so the curve resistance can be neglected. The total train resistance can be rewritten as shown in equation 4.14.

$$R_{tot} = R_o + R_t \tag{4.14}$$

Open-air resistance is given by the Davis formula and Strahls Formula and the tunnel resistance is only a function of v^2 and it is the additional resistance that acts on the train as it passes through the tunnel as shown in equation 4.15[7].

$$R_t = f_T.v^2 \tag{4.15}$$

R_t = Tunnel resistance [N]

f_T = Tunnel factor [kg/m]

v = Speed [m/s]

Open air train resistance formula for train NSB Type 73 is represented in equation 4.16[7].

$$R[N] = 9007 + 51.69v[\frac{m}{s}] + 6.203(v[\frac{m}{s}])^2 \tag{4.16}$$

For NSB Type 75, open air train resistance formula is presented in equation 4.17[4].

$$R[N] = 1829[N] + 7.646(v[\frac{m}{s}])^2 \tag{4.17}$$

4.5 Choice of Approach and Use of Data

Depending on the data available from the trains in traffic, different approaches to estimate the tunnel resistance can be followed. The approaches that have been analyzed are summarized in Table 4.1. Note that these specific approaches are chosen as a result of the available input data, and that more variants can be imagined.

Table 4.1: Methods to estimate tunnel resistance

Method	Description	Input Data	Data Set for Analysis
D	Direct estimation from logged acceleration.	v(t), a(t)	Maximum traction phase
VF1	Indirect estimation by fitting the calculated velocity using maximum traction force.	v(t), $F_{trac}^{std}(v)$, functional form of R(v)	Maximum traction phase
VF2	Indirect estimation by fitting the calculated velocity using traction force derived from energy consumption data.	v(t), $E_{in}(t)$, functional form of R(v)	Complete data set except braking phase

4.5.1 Direct Estimation Approach

This method is used when acceleration values are also available alongwith the velocity values and during the test run from Stavanger to Kristiansand, acceleration values were also logged. By inserting traction force, gradient force and net force values in equation 4.5, resistance values are estimated as shown in Figure 4.2.
Total resistance is estimated using equation 4.5 and open resistance value is subtracted to get the tunnel resistance.

Estimation of Tunnel Factor

Tunnel factor is estimated by extracting the tunnel resistance from total resistance and is done by subtracting the value of open resistance from total resistance. Eqution 4.16 is used to estimated the open resistance for NSB Type 73. Tunnel resistance is then plotted against square of velocity and curve fitting is being done to estimate the tunnel factor (f_T).

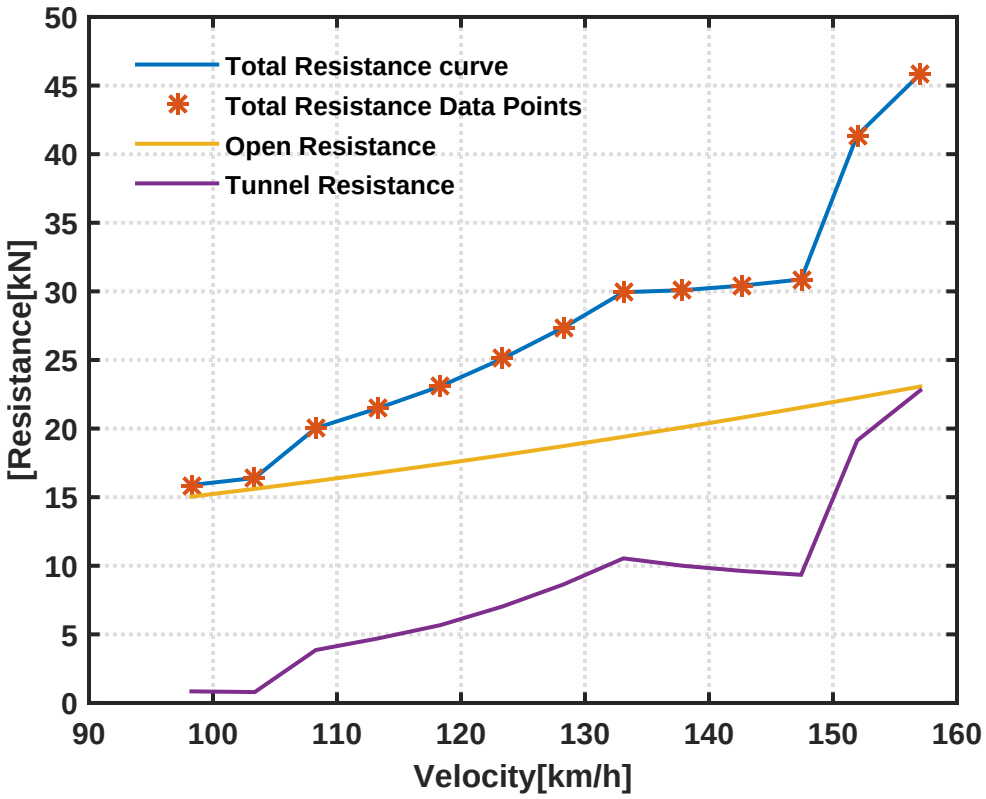

Figure 4.2: Direct estimation approach for Teloc data

4.5.2 Velocity Fitting Approach

In this method, calculated velocity profile is fitted on the measured velocity profile by minimizing the difference between these velocity values using equation 4.9. Numerical integration is performed to estimate total resistance coefficient C. It is being performed by using both Teloc data and energy data.

Using Maximum Traction

Both Teloc 2000 and 2500 data is used to perform numerical integration for estimation of total resistance coefficient. Traction force values are the same as NSB applies for run time calculations corresponding to maximum traction force (240 kN) and maximum power output (4500 kW)[2]. Numerical integration is performed using $Python$ together with a least square optimization from $scipy$ in a program code developed by NSB. As the running resistance can be

represented by equation 4.8 [5][14][17][11], thus equation 4.6 can be re-written as:

$$a = \frac{F_{tr} - mgp - (A + Bv + Cv^2)}{m\rho} \tag{4.18}$$

In this approach, values used for A and B for NSB Type 75 are taken from the Stadler energy consumption report[4] and for Type 73 from Open Track manual [7] and C is estimated by performing the numerical integration of equation 4.18. Value of C is extracted at a point the estimated velocity curve fits well the measured velocity curve as represented in Figure 4.3.

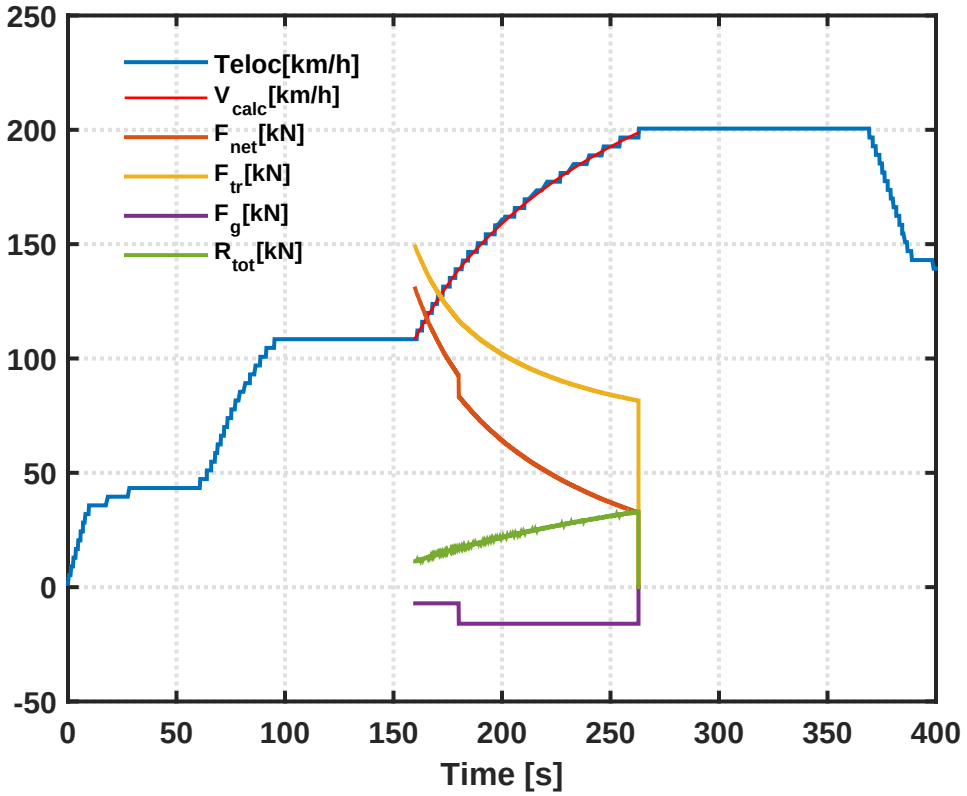

Figure 4.3: Velocity fitting method for Teloc data

In the Figure 4.3, blue curve represents the velocity curve plotted by extracting the values from Teloc and red curve is the fitting velocity curve and is named as measured velocity. Curve fitting is done only for those accelerating sections that are present inside the tunnels. The brown, yellow, purple and green curves represent the net force, traction force, gradient force and net resistance with increase in velocity respectively.

Using Traction Force from Energy Data

The procedure used to estimated the net resistance is the same as peroformed in the method using maximum traction force. The only difference is in the procedure to evaluate the traction force values. In this approach, traction force is estimated from energy data by using equation 4.11. Using new traction values, curve fitting is done again to estimate resistance coefficient C and is shown in Figure 4.4.

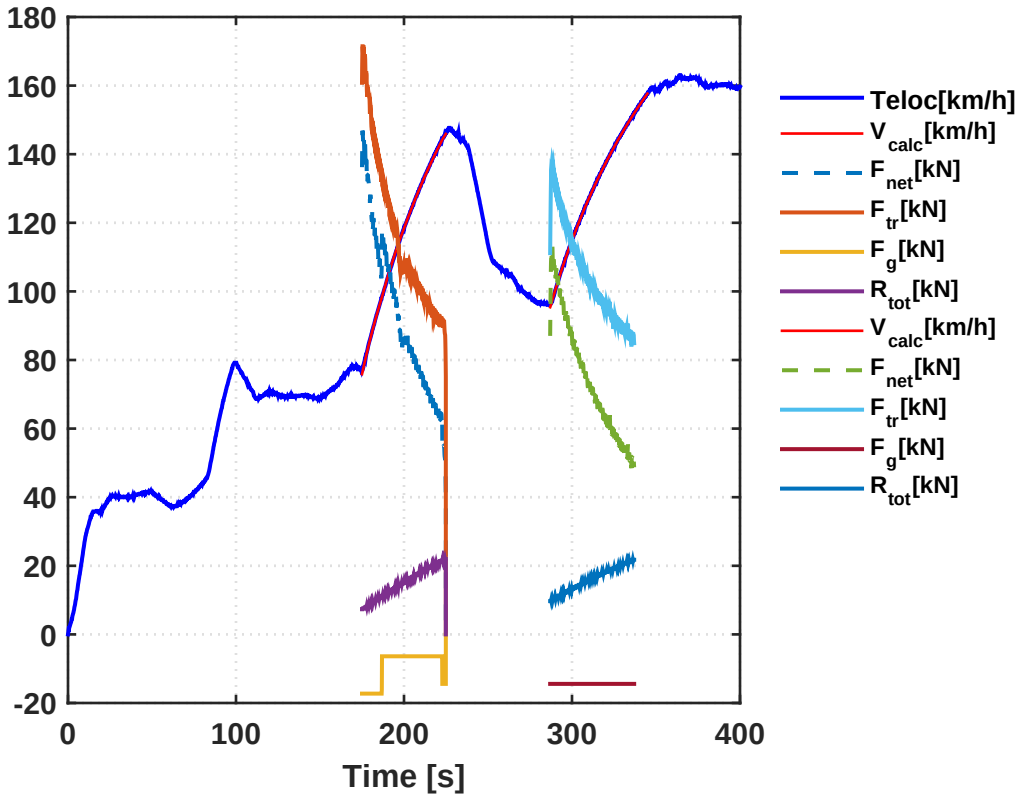

Figure 4.4: Velocity fitting method for energy data

In the figure, curve fitting is done for two accelerating sections because both these sections are present inside the tunnel. Alongwith the increase in velocity, variations in net force, gradient force, traction force and net resistance can be seen in the Figure 4.4.

5. Results and Discussions

In this chapter, tunnel factor is estimated using direct and velocity fitting aprroaches and estimated value of tunnel factor is used to measure tunnel resistance. Tunnel resistance is plotted against velocity and is demonstrated for each of the two methods.
Tunnel factor is calculated using equation 5.1.

$$f_T = C - C_o \tag{5.1}$$

where

f_T = Tunnel factor

C = Total resistance coefficient depending on aerodynamics

C_o = Open air resistance C coefficient

Value of C is estimated using $Python$ program code developed by NSB and C_o is taken from the already developed equations [7][18] for open air resistance calculations for NSB Types 73 and Type 75. Only parameter C is estimated because its value mainly depends on aerodynamics which changes significantly inside the tunnels [19]. Parameters A and B are mainly mass dependent properties [19][14] and changes in aerodynamics of a train does not affect significantly these parameters.

5.1 Direct Method

In direct method, values for coefficients A and B are taken from Strahl/Sauthoff formula [7] and the coefficient C is estimated for Kvienshei, Siratunnelen, Gylandtunnelen, Hægebostad and Tronåstunnelen by plottinng curve fits.

The tunnel factor is calculated using the C coefficient for these five tunnels and the resulting values are displayed in Table 5.1.

Table 5.1: Tunnel factors using Direct Approach

Tunnels	Kvineshei	Siratunnelen	Tronåstunnelen	Gylandtunnelen	Hægebostad
f_T **[kg/m]**	7.4	9.8	9.9	2.1	4.2

Tunnel factors are approximated by plotting curve fits with the values ranging from 2.1 to 9.9 kg/m. The curve fits plotted to measure the tunnel factor are displayed in the Figures 5.1, 5.2, 5.3, 5.4 and 5.5. Figures above show that there are significant variations between tunnel factors. This is because the curve fits plotted on tunnel resistance curves do not fit well due to a low number of data points available and negative values of tunnel resistance for all tunnels except Kvineshei.

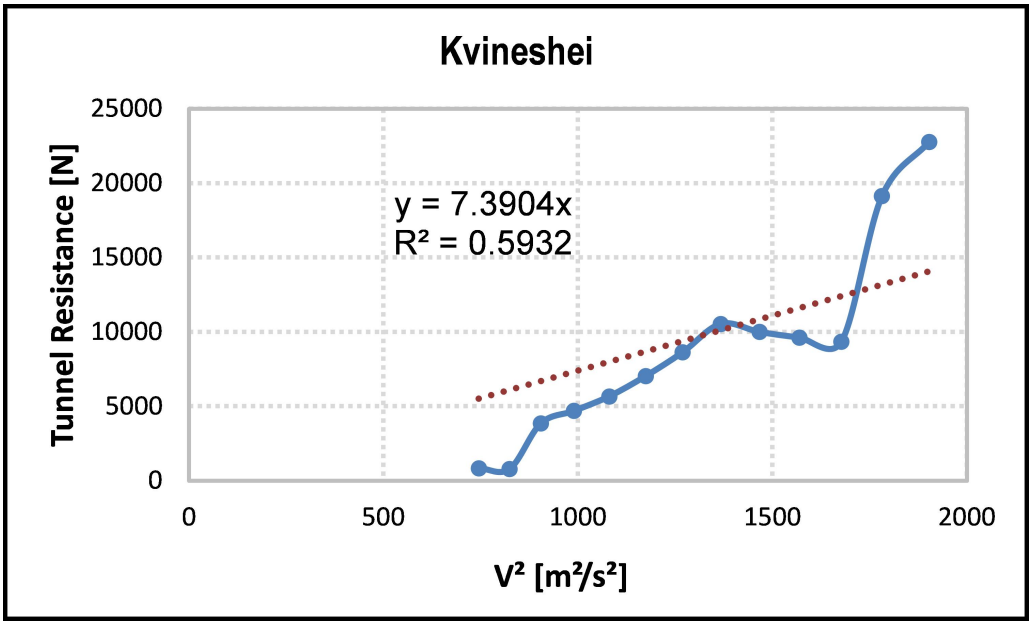

Figure 5.1: Curve fitting for Kvineshei

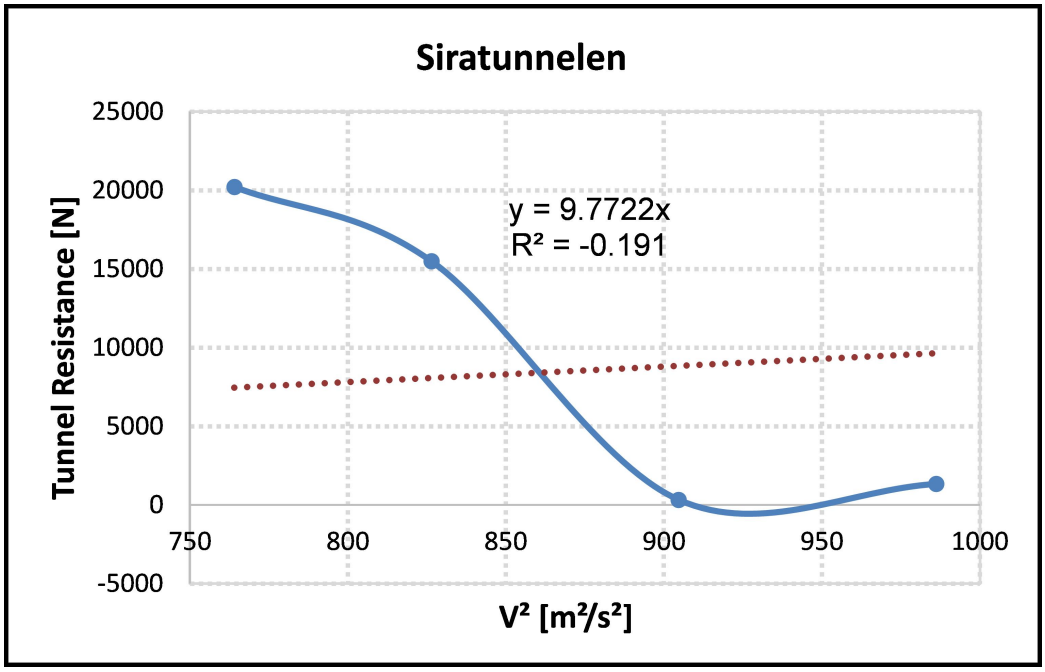

Figure 5.2: Curve fitting for Siratunnelen

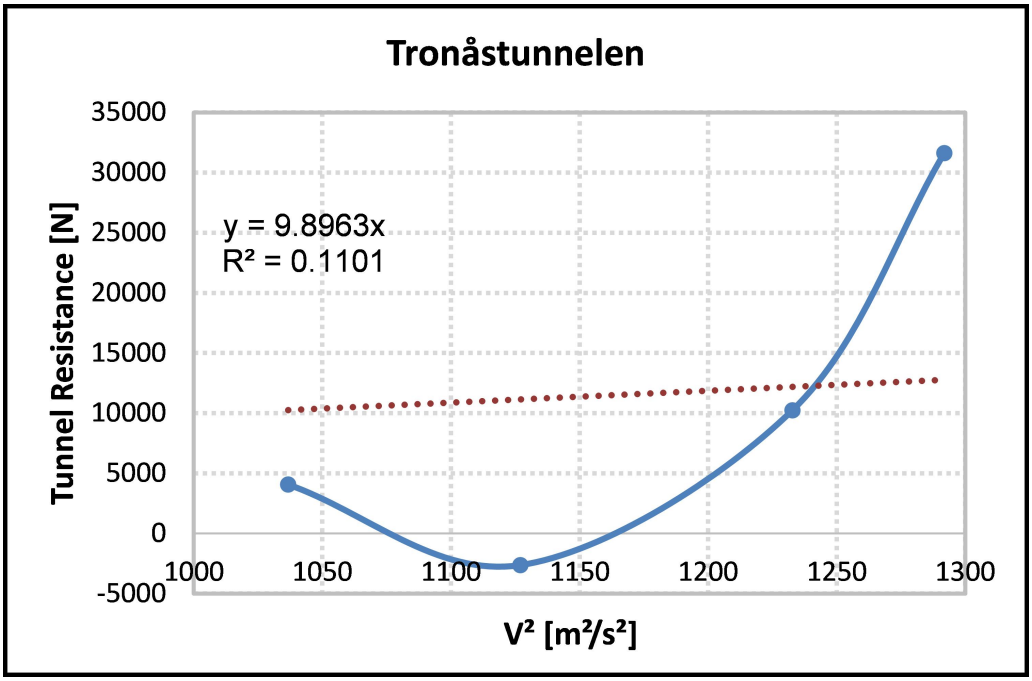

Figure 5.3: Curve fitting for Tronåstunnelen

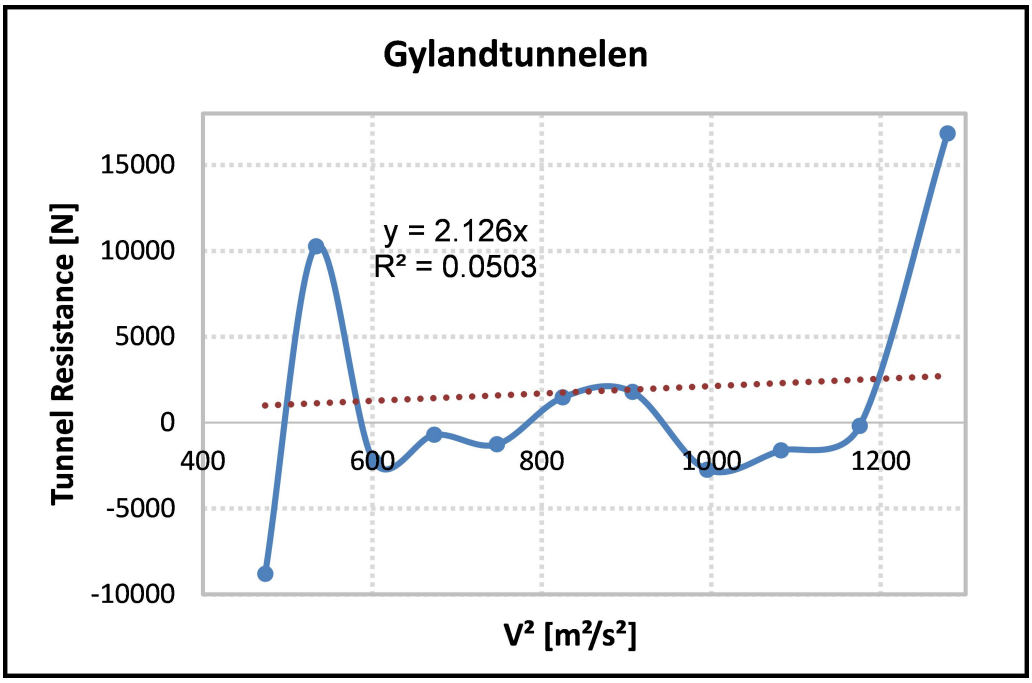

Figure 5.4: Curve fitting for Gylandtunnelen

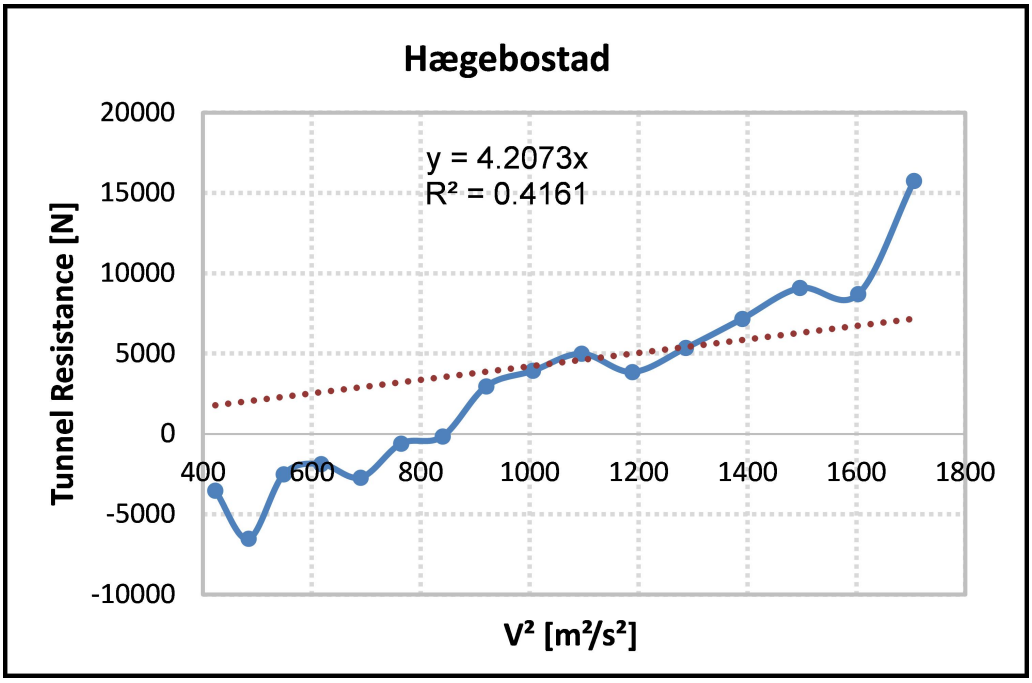

Figure 5.5: Curve fitting for Hægebostad

Tunnel resistance is measured using these tunnel factors and is shown in Figure 5.6. This figure represents resistances for each velocity range for different tunnels. The velocities range as shown in the figure varies for each tunnel because these are the actual velocities with which a train crosses the tunnel. Results show that the tunnel factor is the highest for Tronåstunnelen and therefore resistance experienced by the train is the highest, and for Hægebostad, tunnel resistance is the lowest because of the lowest value of tunnel factor.

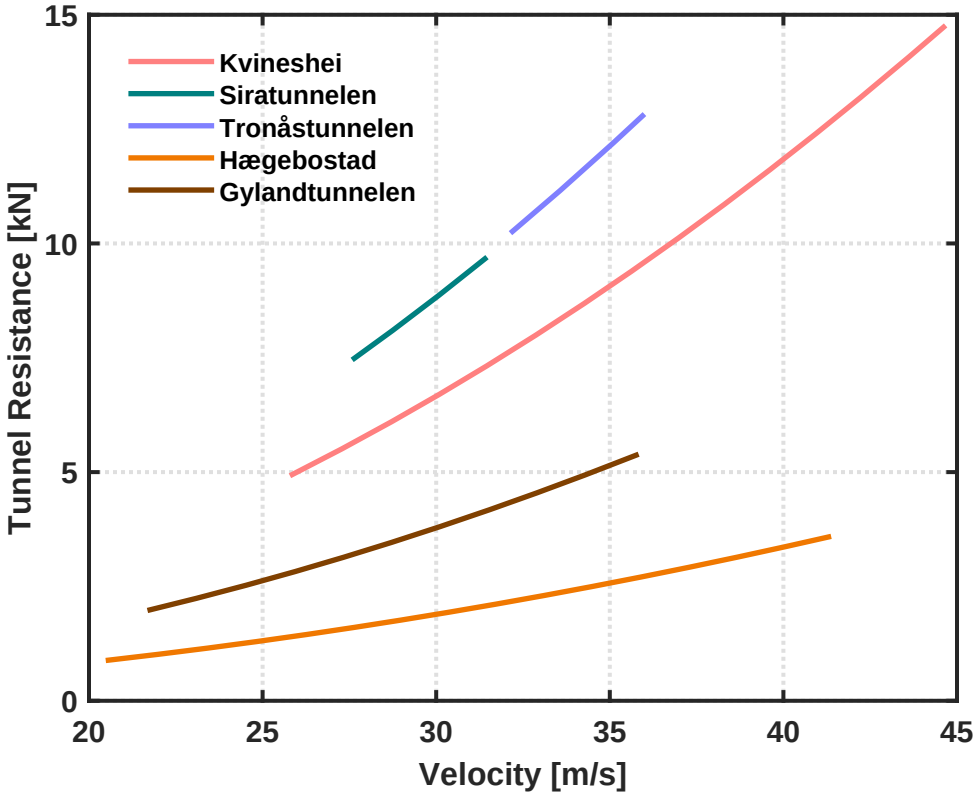

Figure 5.6: Resistance velocity curves from SVG to KRS

5.2 Velocity Fitting Method

In velocity fitting approach, both Teloc and energy data is used to calculate tunnel factor. The tunnel factors and resistance velocity curves are displayed for each data set.

5.2.1 Using Energy Data

Bærumstunnelen is not considered for calculating tunnel factor using energy data because Stadler runs the train in open air between Sandvika and Asker instead of running it through the tunnel, therefore Stadler test runs data is used to calculate the tunnel factor only for four tunnels. The tunnel factors are calculated for both directions between Drammen and Eidsvoll and are displayed in Table 5.2.

Table 5.2: Tunnel factors for tunnels between DRM and EV

Tunnels	f_T $[kg/m]$	
	From DRM to EV	**From EV to DRM**
Romeriksporten	4.1	2.9
Tanumtunnelen	-3.7	5.1
Skaugumtunnelen	1.5	4.6
Lieråsentunnelen	8.9	-

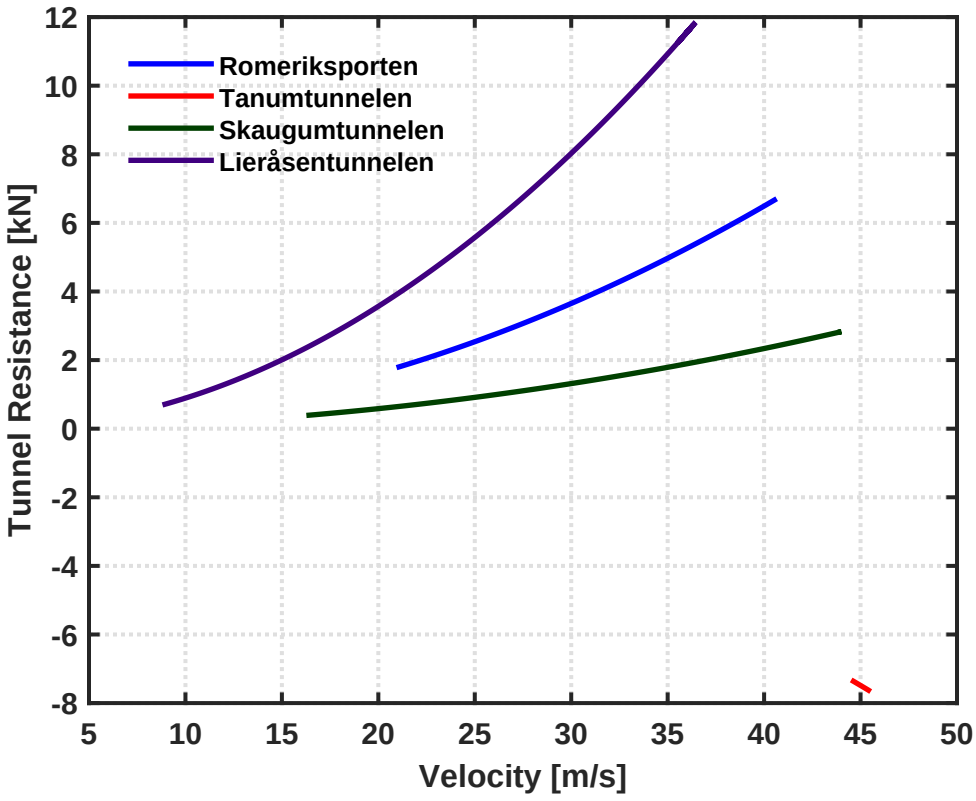

Figure 5.7: Resistance velocity curves for Energy data from DRM to EV

Tunnel factors calculated for a direction from Drammen to Eidsvoll show significant variations ranging between -3.7 and 8.9 kg/m. Due to these variations, there are large differences between resistance velocity curves for each tunnel as shown in Figure 5.7. The figure also depicts that the tunnel resistance for Tanumtunnelen is negative which is practically not possible. The reason for the negative tunnel factor is partly the noise present in the data and partly small sampling velocity range. These are illustrated in Figure 5.7 and 5.9. In turn, tunnel factor for Lieråsentunnelen is the highest among all, and equals 8.9 kg/m. It is becasuse of the smaller cross-section of the Lieråsentunnelen as mentioned in Appendix A.

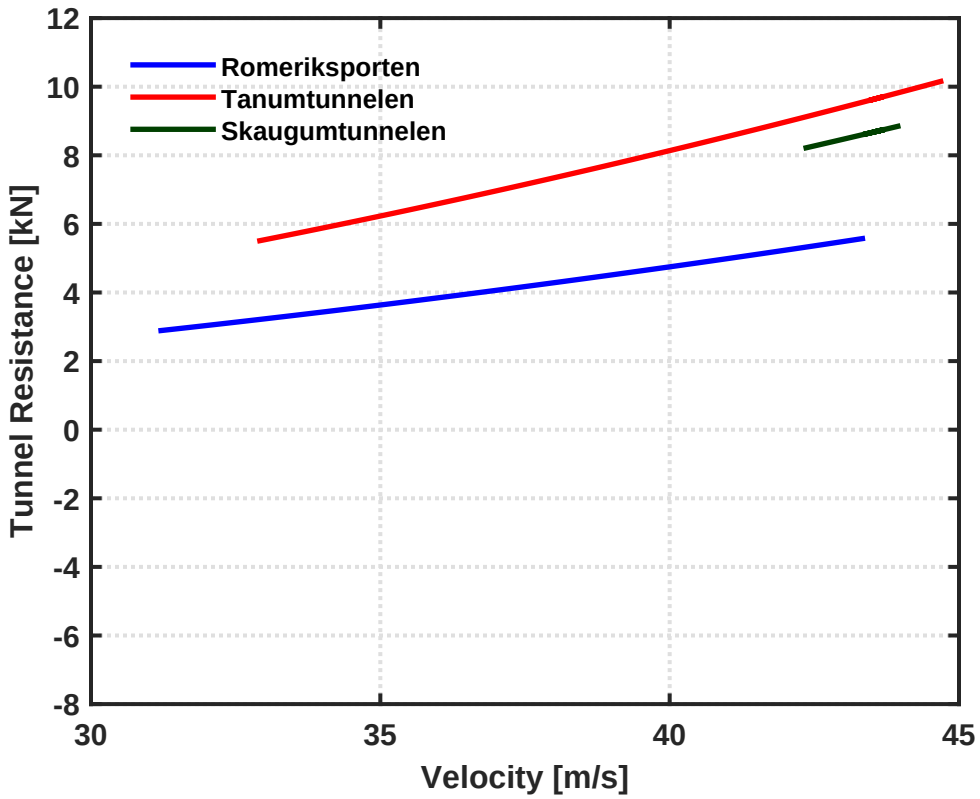

Figure 5.8: Resistance velocity curves for Energy data from EV to DRM

On the other hand, for a direction from Eidsvoll and Drammen, tunnel factors are quite close to each other without any significant variations as shown in Figure 5.8. The smaller variations in tunnel factors for Skaugumtunnelen and Lieråsentunnelen are due to that some noise is still present in the data sets though it is less than for Drammen to Eidsvoll direction.

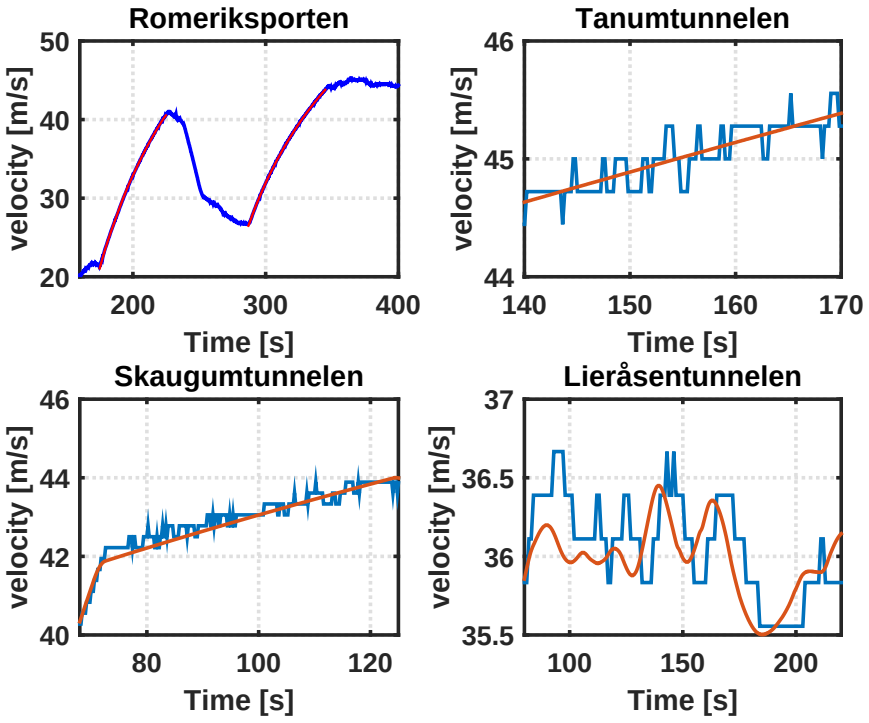

Figure 5.9: Curve fittings for Energy data from DRM to EV

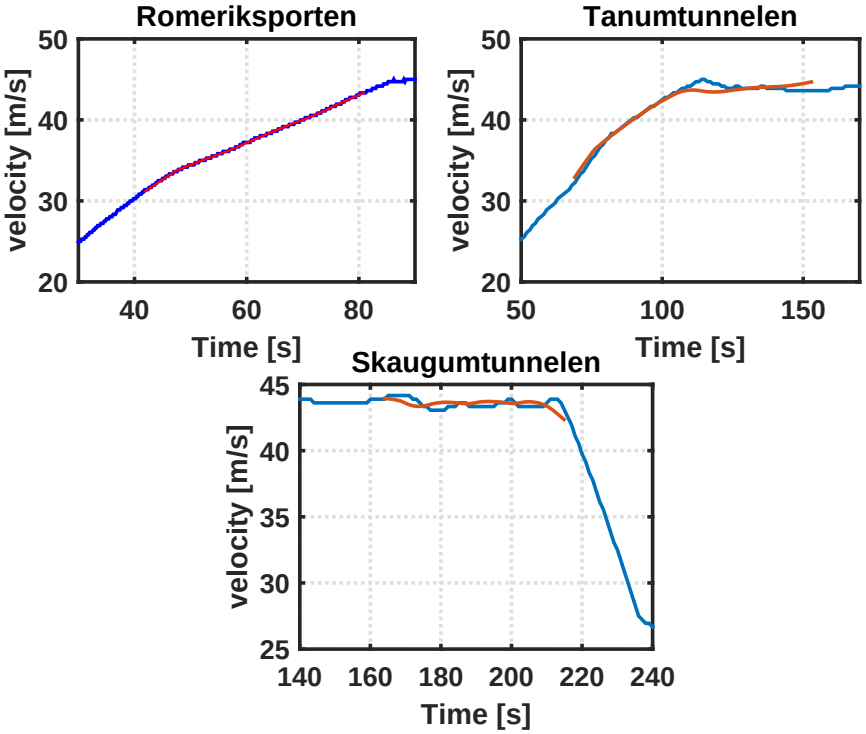

Figure 5.10: Curve fittings for Energy data from EV to DRM

As the quality of data sets is better for Eidsvoll to Drammen direction, having less noise in data and larger sampling velocity range, calculated velocity curves fit well on the measured velocity curves than for Drammen to Eidsvoll direction, which is illustrated in Figure 5.10. Because of this, estimated tunnel factors do not demonstrate large deviations. It should be noted that Lieråsentunnelen is not considered due to the unavailability of data.

5.2.2 Using Teloc Data

Tunnel factors are calculated using equation 5.1 for Teloc 2000 and 2500 data sets and the results are displayed in Tables 5.3 and 5.4. Tunnel factors vary from 2.5 to 7.7 kg/m between Drammen to Eidsvoll and from 5.6 to 9.7 kg/m from Stavanger to Kristiansand.

Table 5.3: Tunnel factors Teloc 2500 data

Tunnels	f_T **[kg/m]**	
	From DRM to EV	**From EV to DRM**
Romeriksporten	2.5	3.2
Bærumstunnelen	3.2	3.4
Tanumtunnelen	-	7.7
Skaugumtunnelen	5.1	-
Lieråsentunnelen	-	4.1

Table 5.4: Tunnel factors Teloc 2000 data from SVG to KRS

Tunnels	Kvineshei	Siratunnelen	Tronåstunnelen	Gylandtunnelen	Hægebostad
f_T **[kg/m]**	9.7	5.9	9.2	5.6	8.4

Using these tunnel factors, tunnel resistance is measured and is plotted against velocities as shown in Figures 5.11, 5.14 and 5.15.

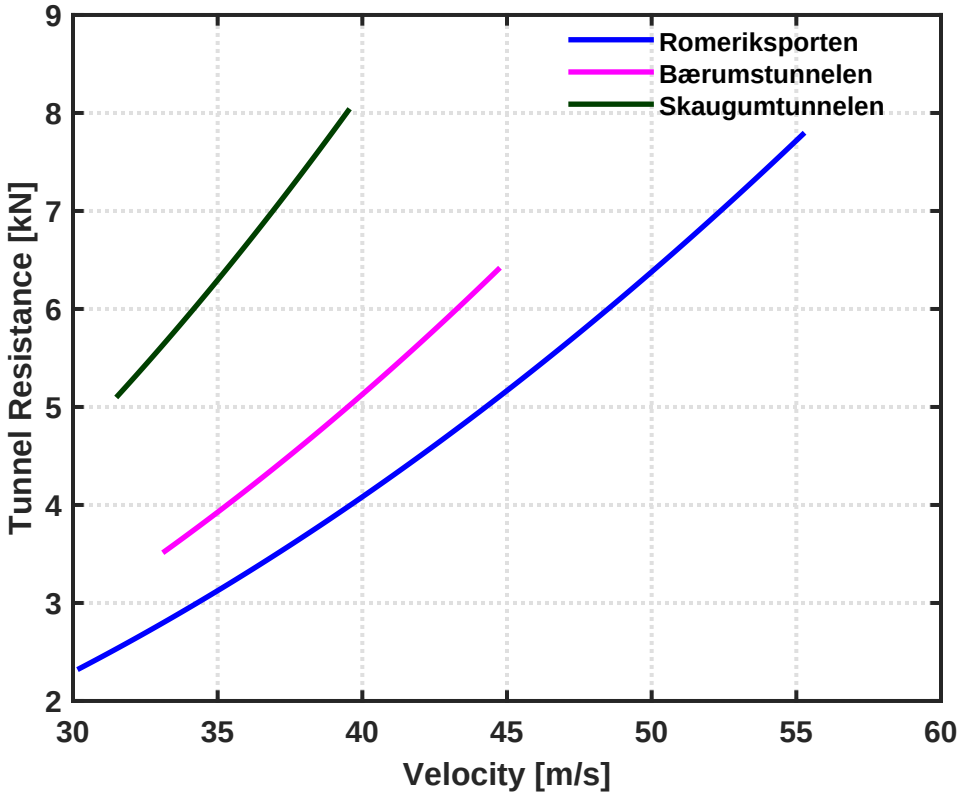

Figure 5.11: Resistance velocity curves for Teloc 2500 from DRM to EV

For a direction from Drammen to Eidsvoll, tunnel factors are not measured for Tanumtunnelen and Lieråsentunnelen. For Tanumtunnelen, velocity remains constant throughout the tunnel section. As the method is applicable only for accelerating sections and velocity curve does not have any accelerating section, therefore no value is estimated for Tanumtunnelen. For Lieråsentunnelen, train experienced signal failure on the day when the test run was performed, so data available for this section is not accurate for estimation of tunnel factor. Curve fits obtained for the three tunnels are displayed in Figure 5.12.

For direction from Eidsvoll to Drammen, tunnel factors do not have large differences except Tanumtunnelen. The highest value of tunnel factor for Tunumtnunelen results from that calculated velocity profile does not fit well on measured velocity profile due to the bigger jumps in the measured velocity curve as illustrated in Figure 5.13. For Skaugumtunelen, tunnel factor is not available because of the constant velocity inside the tunnel.

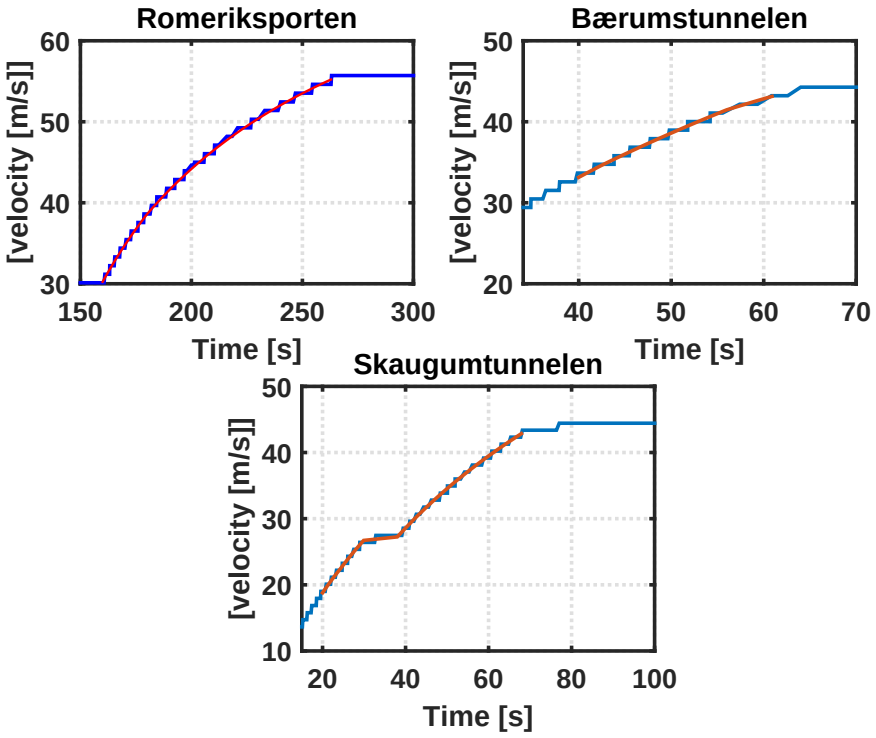

Figure 5.12: Curve fitting from DRM to EV

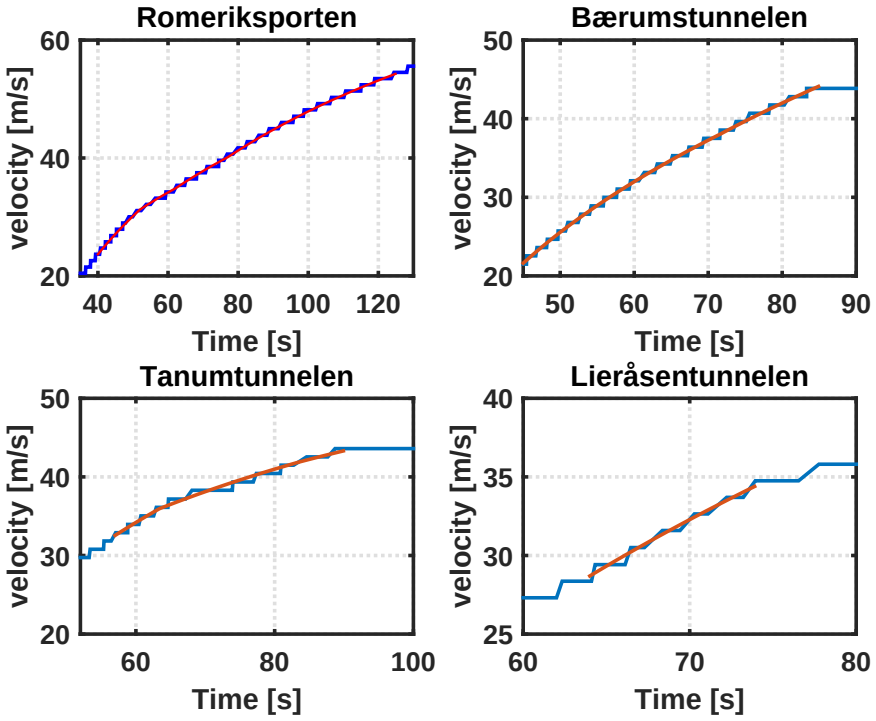

Figure 5.13: Curve fitting from EV to DRM

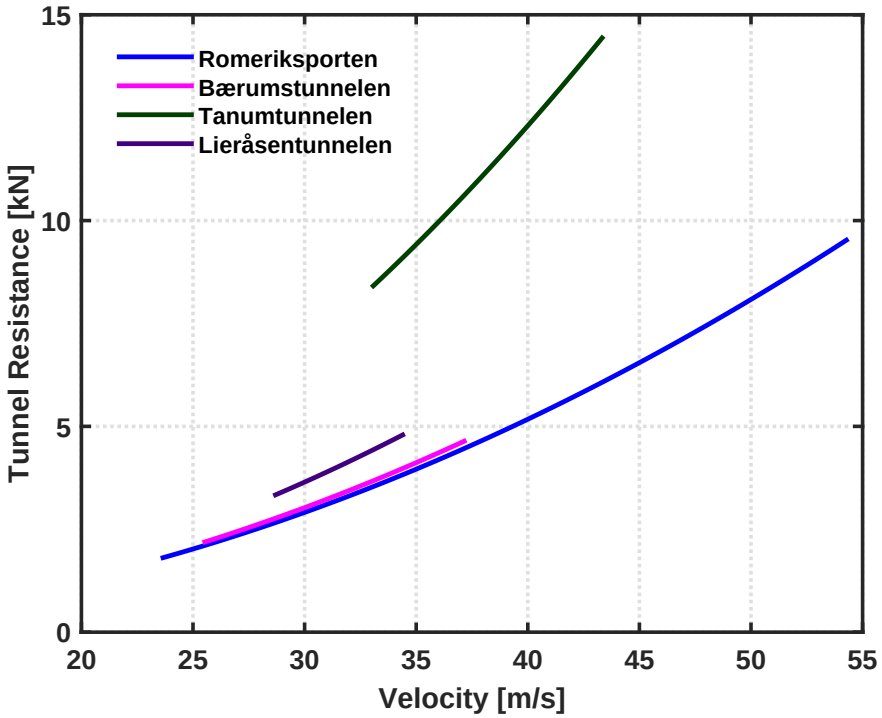

Figure 5.14: Resistance velocity curves for Teloc 2500 from EV to DRM

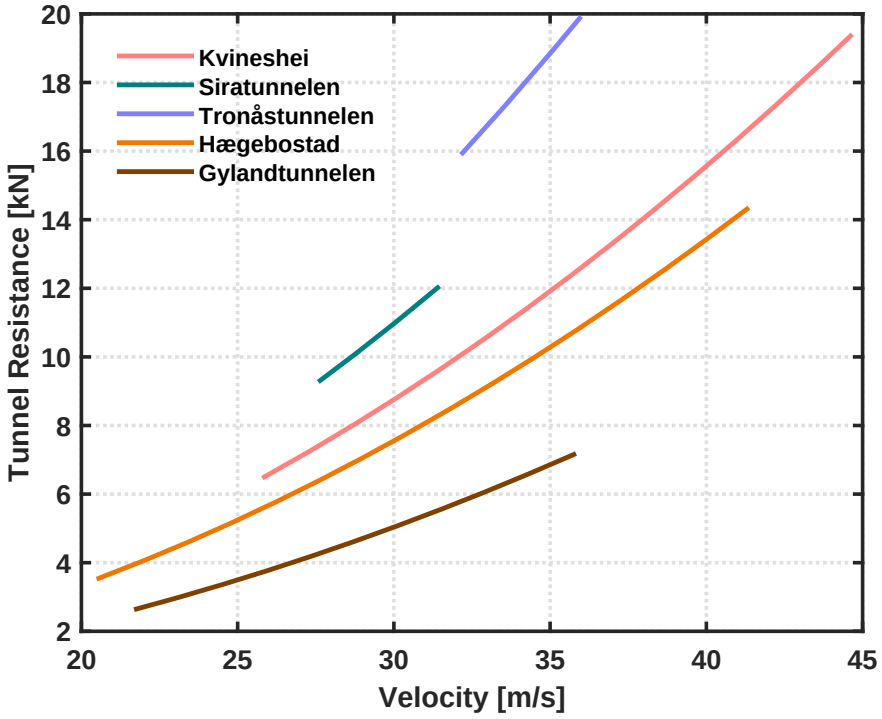

Figure 5.15: Resistance velocity curves for Teloc 2000 from SVG to KRS

Curve fits obtained using velocity fitting approach for Stavanger to Kristiansand data sets are demonstrated in Figures 5.16 and 5.17.

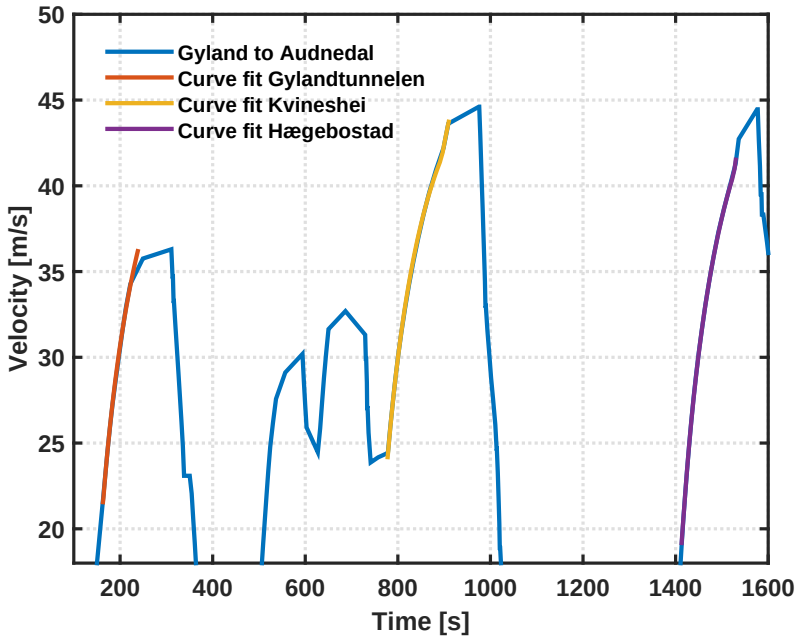

Figure 5.16: Curve fitting for Gylandtunnelen, Kvineshei and Hægebostad

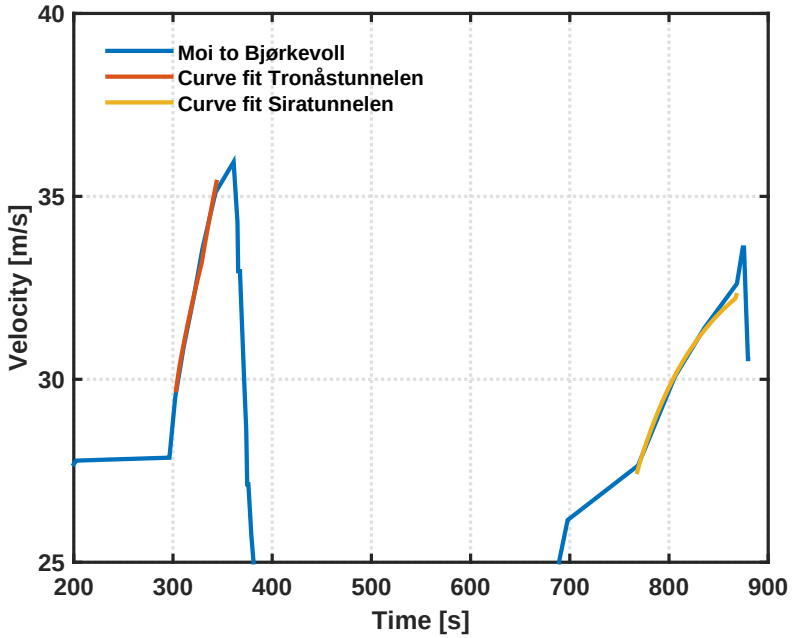

Figure 5.17: Curve fitting for Tronåstunnelen and Siratunnelen

5.3 Comparison on the Basis of Tunnel Factors

Tunnel factors calculated for all data types using both direct and velocity fitting approaches are summarized in Table 5.5. The tunnel factors for Stavanger to Kristiansand are the highest among all the data sets because the tunnels between these two locations are single track having a smaller cross-section area as mentioned in Appendix A. Standard values of tunnel factors used in Viriato 6 and Open Track are given in Table 5.6 [7][18].

Table 5.5: Tunnel factors estimated from direct and velocity fitting approach

Direction	**DRM to EV**	**EV to DRM**	**DRM to EV**	**EV to DRM**	**SVG to KRS**	
Method	**VF1**		**VF2**		**D**	**VF1**
Data Type	**Teloc 2500**		**Energy**		**Teloc 2000**	
Tunnels	**Tunnel Factor (f_T)**					
Romeriksporten	2.5	3.2	4.0	2.9	-	
Bærumtunnelen	3.2	3.3	-	-	-	
Tanumtunnelen	-	7.6	-3.6	5.0	-	
Skaugumtunnelen	5.1	-	1.4	4.5	-	
Lieråsentunnelen	-	4.0	8.9	-	-	
Kvineshei	-	-	-	-	7.4	9.7
Siratunnelen	-	-	-	-	9.8	5.9
Tronåstunnelen	-	-	-	-	9.9	9.2
Gylandtunnelen	-	-	-	-	2.1	5.6
Hægebostad	-	-	-	-	4.2	8.4

Table 5.6: Open Track and Viriato 6 standard tunnel factor values [7][18]

Tunnel Type	**Surface**	**Tunnel Factor (f_T) [kg/m]**
Single Track	Rough	46.38
Single Track	Smooth	23.19
Double Track	Rough	19.28
Double Track	Smooth	9.64

5.3.1 Comparison between Velocity Fitting Approaches

A comparison of velocity fitting one (VF1) and velocity fitting two (VF2) approaches with the standard method used in Open Track and Viriatio 6 is made on the basis of tunnel factors as shown in Figures 5.19, 5.18, 5.21 and 5.20.

Between Drammen and Eidsvoll, tunnel factor is calculated for five tunnels, four tunnels are double track with large cross section whereas Lieråsentunnelen is double track with small cross-section. Tunnel factor calculated from both velocity fitting approaches are lower than the standard tunnel factors used in Open Track and Viriato 6 . Though tunnel factors depend upon type of the tunnel, variations in calculated tunnel factors were observed for the same type of tunnels as well. From Eidsvoll to Drammen variations for both the approaches were approximatley similar while for the reverse direction variations were lower for VF1 as compared to VF2 indicating that Teloc data set is more reliable for estimation of tunnel factors.

In VF1 method as shown in Figures 5.18 and 5.20, velocities are higher than 30 m/s inside the tunnels but in VF2 method, velocities are comparatively less inside the tunnels. Stadler conducted the test runs at lower speed instead of running the trains at maximum allowed speed, therefore velcities are low in VF2 method.

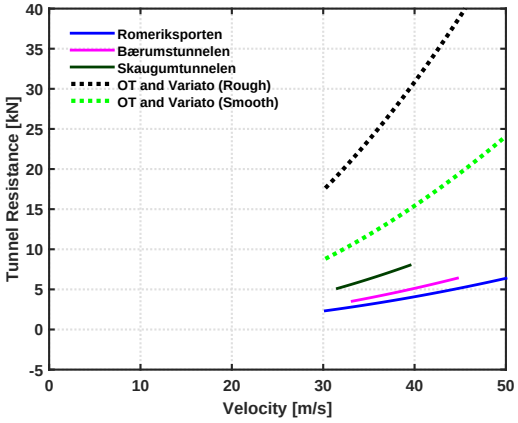

Figure 5.18: VF1 Method from DRM to EV

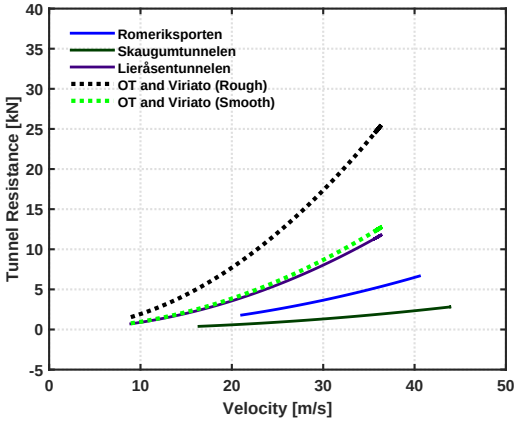

Figure 5.19: VF2 Method from DRM to EV

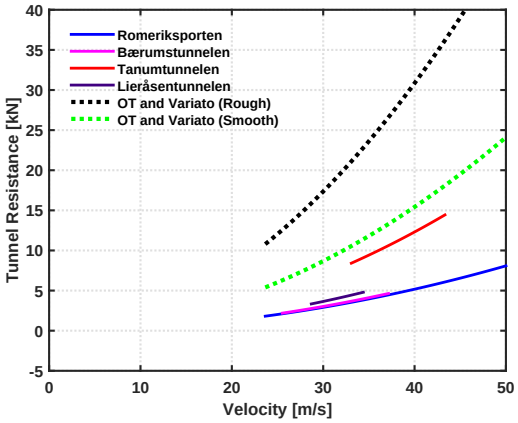

Figure 5.20: VF1 Method EV to DRM

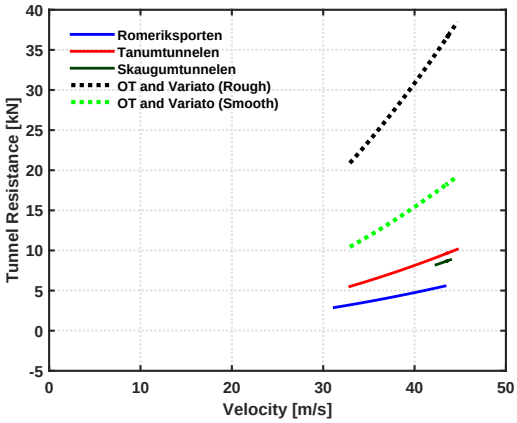

Figure 5.21: VF2 Method EV to DRM

5.3.2 Comparison between Velocity Fitting and Direct Approach

For Teloc 2000 data, tunnel factors are calculated using both velocity fitting and direct approaches. These test runs were conducted from Stavanger to Kristiansand on NSB Type 73. Tunnel factors estimated for these runs are greater as compared to the test runs conducted between Drammen and Eidsvoll. All the five tunnels between Stavanger and Kristiansand are single track and have smaller cross-section. Therefore, tunnel resistance is higher for these tunnels types and is demonstrated in Figures 5.22 and 5.23.

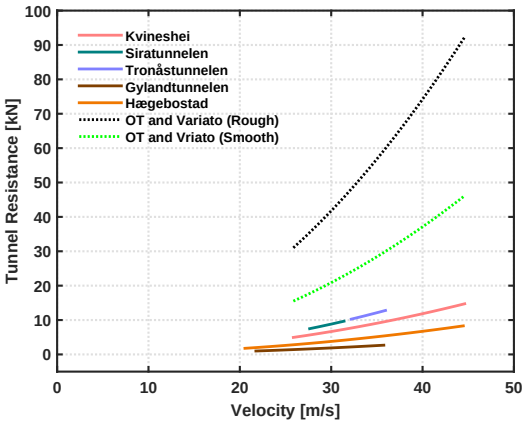

Figure 5.22: Direct approach

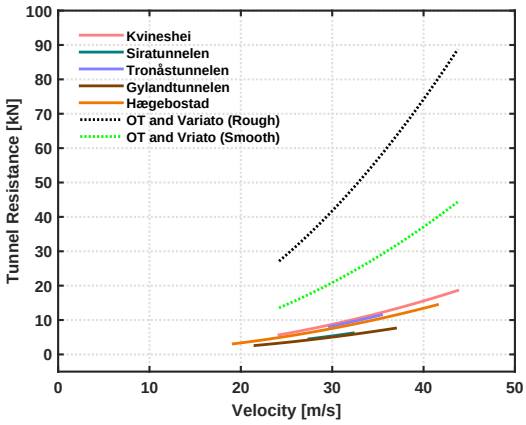

Figure 5.23: Velocity fitting approach

For these tunnels, tunnel factors used in Open Track and Viriato 6 for measuring tunnel resistance are relatively higher but approximately similar differences between estimated values and standard values were observed for both methods. Of these two methods, tunnel resistance estimated by velocity fitting approach showed lower variations and the resistance velocity curves plotted were significantly closer to each other than in direct approach. The inaccuracy in direct approach was caused by availability of fewer data points which lead to inaccurate velocity curve fitting and resulted in large variations in tunnel factor values.

Analysis of the results obtained in this research work with respect to comparison of VF1 and VF2 methods demonstrated that Teloc data is more reliable than energy data. Further usage of Teloc data for direct and velocity fitting approaches showed that velocity fitting method is better as lower variations were observed in calculated tunnel factors. Finally, the tunnel factor values calculated by taking the average of values mentioned in Table 5.5 based on velocity fitting approach are displayed in Table 5.7 and are proposed to use for measuring tunnel resistance more accurately.

Table 5.7: Recommended tunnel factors based on tunnel types

Cross-section	**Tunnel Factor [kg/m]**
Single Track Small Cross-section	7.7
Double Track Small Cross-section	6.4
Double Track Large Cross-section	4.1

6. Conclusion

A new methodology is developed for estimation of running resistance in train tunnel. Train experiences some extra resistance as it enters into the tunnel. Simulation tools Open Track and Viriato 6 use standard equations for calculation of this additional resistance. Studies performed by NSB showed that use of these standard equations result in an overestimation of train resistance, leading to inaccurate estimation of running times and energy consumption. In the current research work, standard methods used in Open Track and Viriato 6 are compared for calculation of tunnel resistance and a new method is developed aiming at more accurate calculation of the tunnel resistance.

Real time data from the test runs performed by NSB and Stadler between Drammen & Eidsvoll and Stavanger & Kristiansand were used. Direct estimation and velocity fittig approaches are developed based on the available data. Teloc data and energy data is used to calculate the tunnel factors using both the approaches. A comparison is made with the standard tunnel factors used in Open Track and Viriato 6 for tunnel resistance estimations.

Three types of tunnels are considered for estmating tunnel resistance. The tunnel factors calculated using direct and velocity fitting approach for these three types of tunnels are less as compared to the standard values used in Open Track and Viriato 6, resulting in more accurate estimation of tunnel resistance and eliminates the problem of overestimation. Velocity fittig method provided more accurate curves fits and yielded lower variations in the tunnel factors. In contrast curve fits in direct approach were relatively less accurate and yielded in higher variations in the tunnel factors. Therefoe, velocity fittig approach is recommended for more accurate calculation of tunnel resistance. As the Teloc data provides the tunnel factors with less variations than energy data, therefore, it is recommended to use the Teloc data to calculate tunnel factor using velocty fitting approach.

After analysig the tunnel factor values using velocity fitting approach, the average tunnel factors are calculated for each tunnel type and are recommended to use for better estimation of tunnel resistance. It is proposed to use 7.7 kg/m for single track tunnels with small cross-section, 6.4 kg/m for double track tunnels with small cross-section and 4.1 kg/m for double track tunnels with large cross-section for more precise calculation of tunnel resistance.

6.1 Future Research

The research can be extended by considering more parameters for calculations and in future work can be done on the following parameters to make tunnel resistance more accurate.

1. Add details to the tunnel resistance formula, e.g. analyse the effect of blockage ratio, tunnel length etc.

2. Discuss tunnel resistance at higher velocities (our measured data ranges from 0-200 km/t), so results can be extrapolated to estimate resistance for high-speed tunnels.

3. Perform a CFD-calculation for the tunnels in question.

Bibliography

[1] (Accessed June 03, 2015). *NSB*. https://www.nsb.no/om-nsb/om-vare-tog.

[2] (Accessed June 06, 2015). *STADLER*. http://www.stadlerrail.com/en/vehicles/flirt/.

[3] (Accessed May 15, 2015). *Jernbaneverkets Kartvisning*. http://customapps2.geodataonline.no/Jernbaneverket/kartinnsyn/.

[4] AG, S. R. (2013). Energy consumption nsb flirt. *Unpublished*.

[5] Boschetti, G. and Mariscotti, A. (2012). The parameters of motion mechanical equations as a source of uncertainty for traction systems simulation. In *Proc. of XX Imeko World Congress, Busan South Korea*.

[6] Chandra, S. and Agarwal, M. M. (2007). *Railway engineering*. Oxford University Press, Oxford.

[7] Daniel Huerlimann, A. B. Open track simulations of railway network. *Unpublished*.

[8] Fairbairn, A. (1995). Tunnel ventilation, including aerodynamics. In *Proceedings of the Institution of Civil Engineers. Civil Engineering*, volume 108, pages 32–41.

[9] Fridstrøm, L. (2013). Norwegian transport towards the two-degree target: Two scenarios. *TOI Report*, (1286/2013).

[10] Lukaszewicz, P. (2001). Energy consumption and running time for trains. *Unpublished dissertation*.

[11] Lukaszewicz, P. (2007). Running resistance-results and analysis of full-scale tests with passenger and freight trains in sweden. *Proceedings of the Institution of Mechanical Engineers, Part F: Journal of Rail and Rapid Transit*, 221(2):183–193.

[12] Nawaz, M.U., O. N. and Hansen, H. (2015). Estimation of tunnel resistance from trains in operation. *To be submitted to Journal of Rail Transport Planning and Managament.*

[13] Pachl, J. (2002). *Railway operation and control.* VTD Rail Publ., Montlake Terrace, Wash.

[14] Profillidis, V. A. (2006). *Railway management and engineering.* Ashgate, Aldershot, Hampshire.

[15] Radosavljevic, A. (2006). Measurement of train traction characteristics. *Proceedings of the Institution of Mechanical Engineers, Part F: Journal of Rail and Rapid Transit*, 220(3):283–291.

[16] Raghunathan, R. S., Kim, H.-D., and Setoguchi, T. (2002). Aerodynamics of high-speed railway train. *Progress in Aerospace sciences*, 38(6):469–514.

[17] Rochard, B. P. and Schmid, F. (2000). A review of methods to measure and calculate train resistances. *Proceedings of the Institution of Mechanical Engineers, Part F: Journal of Rail and Rapid Transit*, 214(4):185–199.

[18] SMA and AG, P. (September 2009). Viriato user's manual. *Unpublished.*

[19] Vardy, A. (1996). Aerodynamic drag on trains in tunnels part 1: synthesis and definitions. *Proceedings of the Institution of Mechanical Engineers, Part F: Journal of Rail and Rapid Transit*, 210(1):29–38.

[20] Vardy, A. and Reinke, P. (1999). Estimation of train resistance coefficients in tunnels from measurements during routine operation. *Proceedings of the Institution of Mechanical Engineers, Part F: Journal of Rail and Rapid Transit*, 213(2):71–87.

A. Appendix

Tunnel Types

Tunnels used to measure tunnel resistance are represented with the pictures. These pictures show the tunnels type and can be used to predict the smoothness and roughness of these tunnels. These pictures are taken at secific distances and are represented along with the tunnel names. The reference point of measuring these distances is the platform of the old Oslo East station, which is 270 m west of the platforms on Oslo S.

The tunnels used in this research work are divided into three categories and are displayed in Table A.1.

Table A.1: Tunnel Categories [3]

Tunnel	Cross-section	Track Type
Romeriksporten	Large	Double
Bærumstunnelen	Large	Double
Tanumtunnelen	Large	Double
Skaugumtunnelen	Large	Double
Lieråsentunnelen	Small	Double
Kvineshei	Small	Single
Siratunnelen	Small	Single
Tronåstunnelen	Small	Single
Hægebostad	Small	Single
Gylandtunnelen	Small	Single

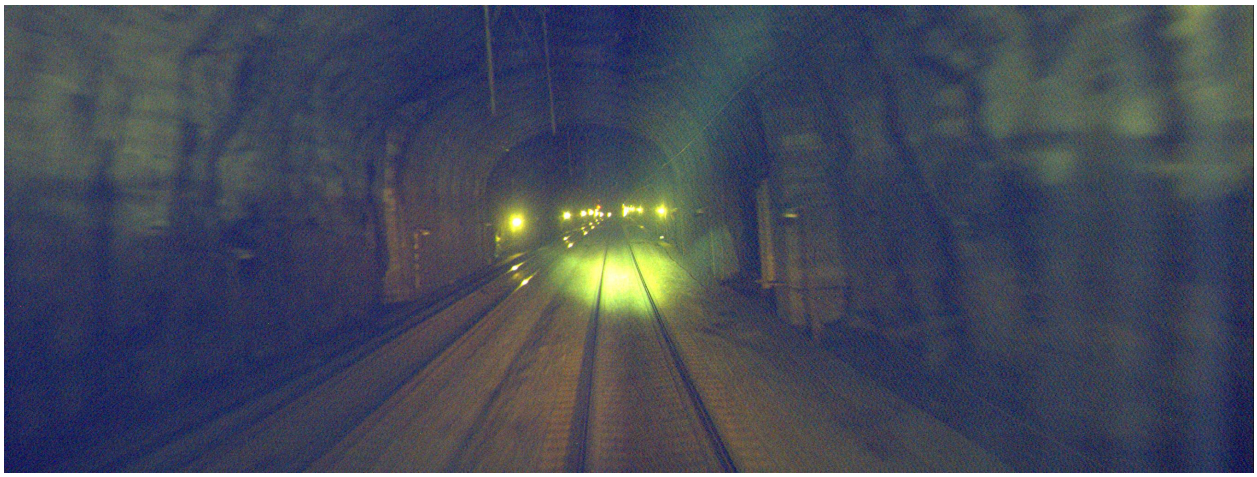

Figure A.1: Romeriksporten at 15.542 km

Figure A.2: Bærumstunnelen at 8.092 km

Figure A.3: Tanumtunnelen at 16.492 km

Figure A.4: Skaugumtunnelen at 19.591 km

Figure A.5: Lieråsentunnelen at 37.038 km

Figure A.6: Siratunnelen at 462.047 km

Figure A.7: Kvineshei at 433.994 km

Figure A.8: Gylandtunnelen 451.209 km

Figure A.9: Hægebostad at 427.116 km

Figure A.10: Tronåstunnelen at 470.747 km